J. Fluid Mech. (2001), *vol.* 431, *pp.* 91–133. Printed in the United Kingdom

Receptivity of boundary layers with distributed roughness to vortical and acoustic disturbances: a second-order asymptotic theory and comparison with experiments

By XUESONG WU

Department of Mathematics, Imperial College, 180 Queens Gate, London SW7 2BZ, UK

(Received 11 February 2000 and in revised form 19 September 2000)

This paper investigates the receptivity of boundary layers due to distributed roughness interacting with free-stream disturbances. Both acoustic and vortical perturbations are considered. An asymptotic approach based on the triple-deck formulation has been developed to determine the initial amplitude of the Tollmien–Schlichting wave to the $O(R^{-1/8})$ accuracy, where R is the global Reynolds number. In the case of vortical disturbances, we show that the dominant contribution to the receptivity comes from the upper deck as well as from the so-called edge layer centred at the outer reach of the boundary layer. It is found that for certain forms of disturbances, the receptivity is independent of their vertical structure and can be fully characterized by their slip velocity at the edge of the boundary layer. A typical case is the vortical disturbance in the form of a convecting wake, for which the same conclusion as above has been reached by Dietz (1999) on the basis of measurements. Our theoretical predictions are compared with the experimental data of Dietz (1999), and a good quantitative agreement has been found. Such a comparison is the first to be made for distributed vortical receptivity. Further calculations indicate that the vortical receptivity in general is much stronger than was suggested previously. In the case of acoustic disturbances, it is found that our first-order theory is in good agreement with experiments as well as with previous theoretical results. But the second-order theory over-predicts, and the possible reasons for this are discussed.

1. Introduction

One of the fundamental questions concerning laminar–turbulent transition in the boundary layer is the so-called receptivity (Morkovin 1969; Reshotko 1976), which refers to the process whereby external disturbances present in the environment (e.g. in a free stream and/or on a wall) excite internal oscillations within the boundary layer. When the free-stream turbulence level is low (below a few per cent), the dominant boundary-layer response is Tollmien–Schlichting (T-S) waves. But high-level free-stream turbulence tends to generate broad-band low-frequency motions, i.e. the so-called Klebanoff modes, which undergo transient growth and may lead to secondary instability. The present paper is concerned with the generation of T-S waves. It is well-known that in a uniform free stream a general unsteady small-amplitude perturbation can be expressed as a superposition of acoustic and vortical modes (and entropy modes if the fluid is compressible) (Kovasznay 1953). The former represents sound waves, while the latter is the vorticity fluctuation being convected

by the free stream and is often referred to as a convecting gust. Because the length and time scales of each mode do not satisfy the dispersion relation of T-S waves, neither of them alone can excite any T-S waves. Therefore the first task of receptivity study is to identify the scale-conversion mechanisms, which 'tune' the time and/or length scales of the external disturbance so as to match those of the T-S waves. The second task of course is to calculate the initial amplitude or equivalently the so-called coupling coefficient.

The major breakthrough came with the seminal papers by Goldstein (1983, 1985) and Ruban (1984), in which several important scale-conversion mechanisms have been identified and quantified. The first of these involves an acoustic disturbance (i.e. a sound wave) interacting with the non-parallel mean flow near the leading edge to excite the so-called Lam–Rott eigensolution, which then undergoes wavelength shortening and finally turns into a T-S wave near the lower branch of the neutral curve (Goldstein 1983). This receptivity, however, turns out to be somewhat weak because the wave may experience considerable decay before reaching its neutral-stability point. A more efficient mechanism was identified independently by Goldstein (1985) and Ruban (1984). It involves the interaction between a sound wave and a rapidly varying mean flow, induced by a small localized roughness on the wall, or by a sudden curvature change (such as the one that occurs at the juncture of the leading-edge ellipse and the straight portion of the plate; see Goldstein & Hultgren 1987). The resulting unsteady forcing can excite a T-S wave if the frequency of the sound and the length scale of the local mean flow are comparable with those of the T-S wave. In the framework of triple-deck theory, the leading-order interaction takes place in the lower deck since both the steady and unsteady perturbations concentrate in that region.

A somewhat similar scale-conversion mechanism operates to generate a T-S wave when a vortical disturbance interacts with a roughness. This has been analysed by Duck, Ruban & Zhikharev (1996), again using a triple-deck formulation. See also Kerschen (1991). The main difference from the acoustic disturbance is that a vortical disturbance does not penetrate into the boundary layer in the sense that its signature is exponentially small there (Gulyaev *et al.* 1989). Thus the dominant interaction now occurs in the upper deck (and also in the so-called edge layer centred at the outer reach of the boundary layer). Since the mean-flow distortion is weaker in the upper deck, the coupling coefficient is found to be a factor $R^{-1/8}$ smaller than that in the corresponding acoustic case, where R is the global Reynolds number. Choudhari (1996) studied the same kind of interaction between a three-dimensional gust and a localized roughness using an approach based on the Orr–Sommerfeld (O-S) equations. His calculations showed that the lower-frequency components of the gust are a more effective T-S wave generator. A quantitative comparison between theory and experiments has not been possible until recently, because earlier experimental investigations (e.g. Kendall 1985, 1990) were conducted in uncontrolled conditions and most information was qualitative. Controlled experiments have been carried out only recently by Dietz (1996, 1998, 1999), who successfully introduced a single-frequency vortical disturbance, a convecting wake, by vibrating a ribbon in the oncoming free stream. His experiments provide for the first time quantitative data about the initial amplitude of the T-S waves due to a convecting gust interacting with a wall roughness element. In the case of localized roughness, Dietz compared his experimental data with the calculations of Choudhari (1996) and also with the prediction by an asymptotic formula of Kerschen (1991). The agreement with the former was reasonable, but the latter turned out to be just about 40% of the measured value. Nevertheless, the

evidence is strong enough to suggest that the basic mechanism proposed in previous theoretical studies is a correct one.

Recently, Wu (1999) proposed a mechanism which is distinct from those mentioned above. It involves the direct interaction between a vortical disturbance and a sound wave of suitable frequencies and wavenumbers so as to achieve scale conversion. Unlike the mechanism in the Goldstein–Ruban theory, the conversion of the external scales does not require any form of non-homogeneity on the wall or in the mean flow, and thus operates even in the simplest flows such as the flat-plate boundary layer.

In addition to the localized roughness, the receptivity due to distributed roughness has also received considerable interest. It has been suggested that this type of roughness is more representative of the practical situation. In theoretical studies, a distributed roughness is conveniently modelled by a wavy wall, while in laboratories it is simulated by arrays of equally spaced isolated roughness elements, placed near the lower branch of the T-S waves that are to be excited (Wiegel & Wlezien 1993; Dietz 1999). Experiments show that the receptivity increases with the number of roughness elements N, but approaches a limit as N becomes sufficiently large ($N = 9 \sim 13$). The final limit corresponds to the case of an infinite wavy wall, and is about one order of magnitude larger than the localized receptivity.

The coupling coefficient of distributed receptivity has been computed by several authors. In the case of an acoustic disturbance, Choudhari (1993) treated the contribution from the distributed roughness as a superposition of that from isolated ones, an idea originated from the work of Tam (1981). Choudhari's analysis is based on the finite-Reynolds-number approach, developed previously by Choudhari & Streett (1992) and Crouch (1992*a*) for the localized receptivity and by Russian researchers (see e.g. Zhigulev & Tumin 1987). A somewhat different finite-Reynolds-number formulation was adopted by Crouch to study the distributed receptivity to acoustic (Crouch 1992*b*) as well as vortical disturbances (Crouch 1994). The key 'device' to determine the T-S waves is an inhomogeneous amplitude equation. This equation, however, was derived in a rather *ad hoc* manner, without making use of a superposition principle (as Choudhari 1993 did) or a solvability condition. A feature of some concern is that in the case of exact resonance, the forcing term in the amplitude equation exhibits a singularity, a second-order pole, at the neutral point of the T-S wave.

In this paper, we shall investigate the distributed receptivity using the high-Reynolds-number approach. The present work was motivated by two facts. First it is desirable to provide a self-consistent mathematical description of the distributed receptivity, in parallel to the work of Goldstein (1985), Ruban (1984) and Duck *et al.* (1996) for the localized roughness. For the distributed receptivity, the non-parallel-flow effect associated with the streamwise variation of the growth rate of the T-S waves plays a key role. In particular, the magnitude of the generated T-S wave is directly related to this effect. This crucial issue can be addressed satisfactorily only in an asymptotic framework. Moreover, in the case of vortical disturbances, the non-parallel effect associated with the thickening of the boundary layer appears at leading order in the edge layer. This effect is completely ignored by the calculations based on the O-S equations, but can be properly taken into account by the high-Reynolds-number approach.

Secondly, for both the acoustic and vortical disturbances, there are well-documented experimental data, notably Dietz (1999) for the vortical receptivity and Wiegel & Wlezien (1993) for the acoustic receptivity. It is now possible to make a detailed quantitative comparison between the theory and laboratory measurements. For this purpose, the asymptotic theory will be extended to the second order, by including

the $O(R^{-1/8})$ correction. Naturally one may be concerned with whether or not the asymptotic approach will be accurate enough for the moderate Reynolds numbers, given that it does not predict the neutral Reynolds number and growth rate accurately. The work of Terent'ev (1981) demonstrates that this approach can be used effectively to study the excitation of T-S waves despite the deficiency mentioned above. The view that the asymptotic approach gives a more accurate prediction for receptivity than for the dispersion was reaffirmed by Choudhari & Streett (1992). Indeed, our final results, (3.124) and (4.38), show that the amplitudes of the T-S waves are not sensitive to the inaccuracy in the predicted neutral Reynolds number.

It should be remarked that the literature on boundary-layer receptivity is rather extensive. Here we have mentioned the contributions that are most relevant to the present work. A more detailed survey was given in a recent paper (Wu 1999), and references to Russian literature on this subject can be found in Duck *et al.* (1996).

The rest of the paper is organized as follows. In § 2, as a first step in formulating the problem, the basic mechanism of the distributed receptivity is described in fairly general terms. The relevant scalings are then introduced so as to develop an asymptotic theory using the triple-deck framework. A wavy wall is used as an idealized model of distributed roughness. The solution of the mean-flow distortion is obtained up to $O(R^{-1/8})$. The receptivity to a vortical disturbance is analysed in § 3. In order to maintain maximum generality, the analysis is carried through without specifying the vertical structure of the gust. The dominant contribution to the receptivity comes from the upper deck as well as the edge layer. The interactions in these two regions are analysed in § 3.1 and § 3.2 respectively. The main layer acts to facilitate the pressure–displacement interplay between the upper and lower decks as in the standard triple deck, and the solution is given in § 3.3. The forcing from the upper and edge layers is transmitted to the lower deck and results in inhomogeneous systems, the solvability conditions of which give rise to the amplitude equations. In § 3.5, we show that the solutions to these equations can be used to determine the T-S wave amplitude up to $O(R^{-1/8})$ accuracy. We demonstrate that in certain conditions, the receptivity is independent of the vertical structure of the gust. Appropriate coupling coefficients are then defined to quantify the receptivity. In §4, we investigate the receptivity to an acoustic perturbation. The leading-order contribution is from the lower deck (§ 4.3). But there is an $O(R^{-1/8})$ contribution from both the upper and main layers, and these are analysed in § 4.1 and § 4.2. The required amplitude equations are derived in § 4.3. Numerical solutions are presented in §5, where the theoretical results are compared with the relevant experiments as well as with previous calculations. The conclusions and implications of the present study are discussed.

2. Formulation and scalings

We consider the two-dimensional incompressible boundary layer over a semi-infinite wavy wall. The oncoming flow is assumed to be uniform with velocity U_∞, perturbed by small-amplitude disturbances, which will be specified later. We define the Reynolds number

$$R = U_\infty l/\nu, \tag{2.1}$$

where l is the typical distance from the leading edge to the location where the receptivity commences, and ν is the kinematic viscosity.

The flow is to be described in the Cartesian coordinate system (x, y, z) with its origin at the leading edge, where x and y are along and normal to the mean position of the

wall respectively, and z is in the spanwise direction; x and z are non-dimensionalized by l and y by $lR^{-1/2}$. The time variable t is normalized by l/U_∞. The velocity (u, v, w) is non-dimensionalized by U_∞, while the non-dimensional pressure p is introduced by writing the dimensional pressure as $(p_\infty + \rho U_\infty^2 p)$, where p_∞ is a constant and ρ is the fluid density.

The basic mechanism of the distributed receptivity is well understood from the physical point of view, and can be explained in fairly general terms as follows. Suppose first that the dispersion relation of the T-S wave is

$$\Delta(\hat{\omega}_{TS}, \hat{\alpha}_{TS}; x) = 0, \tag{2.2}$$

which relates the frequency $\hat{\omega}_{TS}$ and the wavenumber $\hat{\alpha}_{TS}$ at a given location x, the dependence on which is parametric. In general for a given frequency $\hat{\omega}_{TS}$, the wavenumber $\hat{\alpha}_{TS} = \hat{\alpha}_r + \mathrm{i}\hat{\alpha}_i$ is a complex number except at the neutral position x_0.

In the case of an acoustic disturbance, the pressure fluctuation in the free stream drives an oscillatory flow near the wall. In the incompressible limit, this flow is proportional to $\mathrm{e}^{-\mathrm{i}\hat{\omega}_s t}$. On the other hand, the wall roughness induces a steady mean flow proportional to $\mathrm{e}^{\mathrm{i}\hat{\alpha}_w x}$, where $\hat{\omega}_s$ and $\hat{\alpha}_w$ are the frequency of the sound and the wavenumber of the roughness respectively. The interaction between the two generates a forcing term proportional to $\mathrm{e}^{\mathrm{i}(\hat{\alpha}_w x - \hat{\omega}_s t)}$. Now if

$$\hat{\omega}_s = \hat{\omega}_{TS}, \quad \hat{\alpha}_w \approx \mathrm{Re}\,(\hat{\alpha}_{TS}), \tag{2.3}$$

the response to the forcing would be similar to, but not exactly the same as, the T-S wave when $x \neq x_0$. But when $x \approx x_0$, the relations in (2.3) imply that a resonance occurs between the forcing and the T-S wave, leading to the generation of the latter. Mathematically, the resonance means that in order for the inhomogeneous system at the quadratic order to have an acceptable solution, the T-S wave solution must be included in the expansion at a suitable lower order.

In the case of a vortical disturbance (gust), the velocity (and vorticity) fluctuation in the free stream is proportional to $\exp(\mathrm{i}(\hat{\alpha}_c x - \hat{\omega}_c t))$. Since $\hat{\alpha}_c = \hat{\omega}_c$, there is no pressure fluctuation at leading order, and as a result a vortical disturbance does not penetrate into the boundary layer. But as in the case of the localized receptivity (cf. Duck *et al.* 1996), an interaction with the mean-flow distortion takes place in the outer reach of the boundary layer, producing a forcing proportional to $\exp(\mathrm{i}(\hat{\alpha}_w + \hat{\alpha}_c)x - \mathrm{i}\hat{\omega}_c t)$. A resonance occurs in the vicinity of the lower-branch neutral point x_0 if

$$\hat{\omega}_c = \hat{\omega}_{TS}, \quad \hat{\alpha}_w + \hat{\alpha}_c \approx \mathrm{Re}\,(\hat{\alpha}_{TS}). \tag{2.4}$$

It is noted that for a gust or a sound wave of a given frequency, there exists a unique value of $\hat{\alpha}_w$ to satisfy exactly the second relation in (2.3) or (2.4). Conversely, a roughness of a given wavelength requires the gust or sound to have a particular frequency in order to have an exact resonance. In controlled experiments, one usually imposes $\hat{\alpha}_w$ and varies $\hat{\omega}_c$ (or $\hat{\omega}_s$) over a range in which the second relation in (2.3) or (2.4) is satisfied only approximately. T-S waves may still be generated in this more general case, but have a reduced magnitude. Such a tuned response to the forcing frequency is an important feature of the distributed receptivity, and can be described by introducing an appropriate detuning parameter (see later).

To calculate the coupling coefficient in each case, we shall develop an asymptotic theory based on the triple-deck formalism; so we assume that $R \gg 1$. For a lower-branch T-S wave, its frequency and wavenumber scale with the Reynolds number as

$$\hat{\omega}_{TS} = R^{2/8}\omega, \quad \hat{\alpha}_{TS} = R^{3/8}\alpha.$$

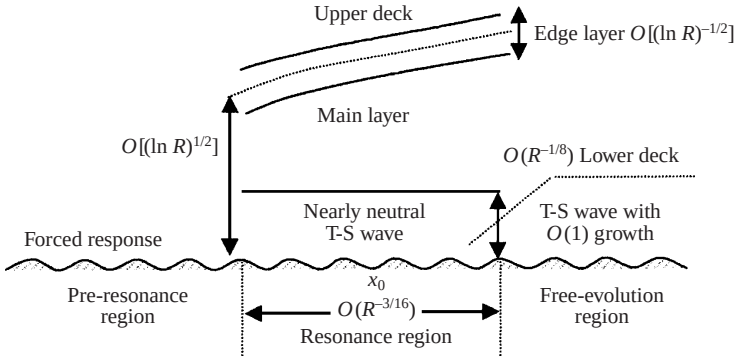

FIGURE 1. Illustration of the receptivity process and the flow structure for the vortical receptivity.

Since the generated T-S wave inherits the frequency of the sound wave or gust, we have

$$\hat{\omega}_s = \hat{\omega}_c = \hat{\omega}_{TS} = R^{2/8}\omega, \quad \hat{\alpha}_c = R^{2/8}\alpha_c.$$

Though $\alpha_c \equiv \omega$, we shall retain the identity of α_c for book-keeping purpose. The resonant condition (2.3) or (2.4) shows that the wavenumber of the wall roughness must scale as

$$\hat{\alpha}_w = R^{3/8}\alpha_w.$$

It is also convenient to introduce the faster variables

$$\bar{t} = R^{2/8}t, \quad \bar{x} = R^{3/8}x, \quad \bar{z} = R^{3/8}z, \tag{2.5}$$

and a small parameter

$$\epsilon = R^{-1/8}.$$

The important site of the receptivity process is the neutral point x_0 of the T-S wave, since the resonance condition can only be met there. Upstream of x_0, the quadratic roughness–gust or roughness–sound interaction generates a small-amplitude response, which is regular. But as x_0 is approached, the forced response tends to infinity (i.e. becomes singular), and takes on the characteristics of the T-S wave. In order to describe this crucial process of the forced response evolving into the T-S wave after going through the resonance, it is necessary to consider the $O(R^{-3/16})$ neighbourhood of x_0, where the non-parallel-flow effect becomes important in the sense that the variation of both the growth rate and the amplitude occurs at the same scale (Ruban 1983, Hall & Smith 1984). We introduce

$$x_1 = (x - x_0)/R^{-3/16}. \tag{2.6}$$

The amplitude of the T-S wave will be a function of x_1, and matches to the forced response upstream as $x_1 \to -\infty$. Sufficiently downstream the T-S wave evolves into the post-resonance region where it acquires an $O(1)$ growth rate. Thus the whole process consists of three stages as is illustrated in figure 1, the most important of which is the resonance region. The key role of the $O(R^{-3/16})$ vicinity of the neutral point in receptivity was demonstrated in Wu (1999). See also Choudhari (1993).

One may note that the distributed receptivity is quite different from the isolated receptivity in terms of physical process as well as the methods used to determine the T-S wave amplitude. An isolated roughness has a continuous spectrum, and when interacting with the unsteady disturbances produces a broad-band response in the

boundary layer. The solution for the response can be expressed as a Fourier integral. The amplitude of the T-S wave is obtained directly by evaluating the residue at the simple pole of the integrand. But for the distributed receptivity, we shall introduce an amplitude function $A(x_1)$ say and derive the equation governing $A(x_1)$. This procedure is similar to that in Wu (1999).

Now it follows from (2.5) and (2.6) that

$$\frac{\partial}{\partial t} \to R^{2/8}\frac{\partial}{\partial \bar{t}}, \quad \frac{\partial}{\partial x} \to R^{3/8}\frac{\partial}{\partial \bar{x}} + R^{3/16}\frac{\partial}{\partial x_1}, \quad \frac{\partial}{\partial z} \to R^{3/8}\frac{\partial}{\partial \bar{z}}. \tag{2.7}$$

The mean flow is taken to be the Blasius boundary layer, the profile of which is $U_B(y)$. As $y \to 0$,

$$U_B(y) \to \lambda y$$

where the skin friction

$$\lambda = \chi x^{-1/2} \quad \text{with } \chi \approx 0.332. \tag{2.8}$$

We further expand λ about x_0, the location where the T-S wave becomes neutral,

$$\lambda = \lambda_0 + R^{-3/16}\lambda_1 x_1, \quad \text{with } \lambda_1 = -\tfrac{1}{2}\chi x_0^{-3/2}. \tag{2.9}$$

Since the length scale l (see (2.1)) is taken to be the distance of the neutral point to the leading edge, x_0 will be assigned the value of unity.

For the triple deck to be applicable, the dimensional height of the wall waviness, h^*, must be of $O(R^{-5/8}l)$ or smaller, and so we may write $h^*/l = R^{-5/8}h$ with $h = O(1)$ or smaller. For simplicity, we shall assume that the mean-flow distortion, and the vortical and acoustic disturbances are all of sufficiently small magnitude that their self-nonlinearities can be ignored. Formally this requires that

$$h \ll R^{-1/8}, \quad \epsilon_c \ll R^{-1/8}, \quad \epsilon_s \ll R^{-1/8}, \tag{2.10}$$

where ϵ_c and ϵ_s stand for the amplitudes of the streamwise velocities of the sound and gust respectively. For such small-amplitude waviness, there is no loss of generality to assume that the distribution of the roughness is purely sinusoidal since a more general periodic pattern can be decomposed into Fourier series. Thus we take the wall position to be given by

$$y = R^{-1/8}F_w h(\mathrm{e}^{\mathrm{i}\alpha_w \bar{x}} + \text{c.c.}), \tag{2.11}$$

where F_w is an order-one parameter representing the coefficient of the first term in the Fourier series, and c.c. stands for complex conjugate.

In order to develop a second-order asymptotic theory which can predict the initial amplitude of the T-S wave with $O(R^{-1/8})$ accuracy, it is necessary (i) to retain the $O(R^{-1/8})$ correction to the leading-order forcing, and (ii) to take into account the correction arising from the higher-order modification to the dispersion relation of the T-S wave. In particular, the latter solution must be obtained up to $O(R^{-2/8})$ so that the detuning effect can be described to the required order of accuracy.

As the analysis is lengthy, readers who are more interested in the physical mechanisms and the final quantitative predictions rather than mathematical technicalities could go directly to § 3.5 and the end of § 4, where we give the final results, (3.124) and (4.38), the coupling coefficients for the acoustic and vortical receptivities respectively.

2.1. *The mean-flow distortion*

In the main part of the boundary layer, the mean-flow distortion due to the wavy wall is a small perturbation to the Blasius profile $(U_B, R^{-1/2}V_B)$, that is

$$(U, V, P) = (U_B + \epsilon h U_M,\ R^{-1/2}V_B + \epsilon^2 h V_M,\ \epsilon^2 h P_M),$$

where (U_M, V_M, P_M) expand as

$$\left.\begin{aligned} U_M &= \{U_M^{(1)} + \epsilon U_M^{(2)} + \cdots\}\,\mathrm{e}^{\mathrm{i}\alpha_w \bar{x}} + \text{c.c.} + O(h)\ldots, \\ V_M &= \{V_M^{(1)} + \epsilon V_M^{(2)} + \cdots\}\,\mathrm{e}^{\mathrm{i}\alpha_w \bar{x}} + \text{c.c.} + O(h)\ldots, \\ P_M &= \{P_M^{(1)} + \epsilon P_M^{(2)} + \cdots\}\,\mathrm{e}^{\mathrm{i}\alpha_w \bar{x}} + \text{c.c.} + O(h)\ldots\ . \end{aligned}\right\} \tag{2.12}$$

Here we can ignore the terms proportional to $O(h)$ since $h \ll \epsilon$ as implied by (2.10).

It is well known that the leading-order perturbation has the solution

$$U_M^{(1)} = A_M^{(1)} U_B', \quad V_M^{(1)} = -\mathrm{i}\alpha_w A_M^{(1)} U_B, \tag{2.13}$$

where the constant $A_M^{(1)}$ is to be determined later. The second-order perturbation is governed by

$$\mathrm{i}\alpha_w U_M^{(2)} + V_{M,y}^{(2)} = 0, \tag{2.14}$$

$$\mathrm{i}\alpha_w U_B U_M^{(2)} + U_B' V_M^{(2)} = -\mathrm{i}\alpha_w P_M^{(1)}, \tag{2.15}$$

$$\mathrm{i}\alpha_w U_B V_M^{(1)} = -P_{M,y}^{(2)}, \tag{2.16}$$

which are solved to give

$$V_M^{(2)} = -\mathrm{i}\alpha_w A_M^{(2)} U_B + \mathrm{i}\alpha_w P_M^{(1)} U_B \int^y \frac{\mathrm{d}y}{U_B^2}, \tag{2.17}$$

$$U_M^{(2)} = A_M^{(2)} U_B' - P_M^{(1)} \left\{ U_B \int^y \frac{\mathrm{d}y}{U_B^2} \right\}', \tag{2.18}$$

$$P_M^{(2)} = \tilde{P}_M^{(2)} - \alpha_w^2 A_M^{(1)} \int_0^y U_B^2 \mathrm{d}y, \tag{2.19}$$

where $A_M^{(2)}$ and $\tilde{P}_M^{(2)}$ are constants to be found.

In the upper deck, where $\bar{y} = R^{-1/8} y$, the steady flow can be written as

$$(U, V, P) = (1, 0, 0) + \epsilon^2 h(\bar{u}_M, \bar{v}_M, \bar{p}_M)\,\mathrm{e}^{\mathrm{i}\alpha_w \bar{x}} + \text{c.c.},$$

with

$$(\bar{u}_M, \bar{v}_M, \bar{p}_M) = (\bar{u}_M^{(1)}, \bar{v}_M^{(1)}, \bar{p}_M^{(1)}) + \epsilon(\bar{u}_M^{(2)}, \bar{v}_M^{(2)}, \bar{p}_M^{(2)}) + \cdots. \tag{2.20}$$

The governing equations for $\bar{p}_M^{(j)}$ and $\bar{v}_M^{(j)}$ are

$$\bar{p}_{M,\bar{y}\bar{y}}^{(j)} - \alpha_w^2 \bar{p}_M^{(j)} = 0, \quad \mathrm{i}\alpha_w \bar{v}_M^{(j)} = -\bar{p}_{M,\bar{y}}^{(j)} \quad (j = 1, 2).$$

It follows that $\bar{p}_M^{(j)} = \bar{P}_M^{(j)}\,\mathrm{e}^{-\alpha_w \bar{y}}$ and $\bar{v}_M^{(j)} = -\mathrm{i}\bar{P}_M^{(j)}\,\mathrm{e}^{-\alpha_w \bar{y}}$. The continuity equation gives the streamwise velocities $\bar{u}_M^{(j)} = -\bar{P}_M^{(j)}\,\mathrm{e}^{-\alpha_w \bar{y}}$. The pressure and vertical velocity in the upper deck match their counterparts in the main layer if

$$\bar{P}_M^{(1)} = P_M^{(1)}, \quad \bar{P}_M^{(2)} = \tilde{P}_M^{(2)} - \alpha_w^2 A_M^{(1)} I_2, \tag{2.21}$$

$$P_M^{(1)} = \alpha_w A_M^{(1)}, \quad -\mathrm{i}\bar{P}_M^{(2)} = \mathrm{i}\alpha_w P_M^{(1)} J_\infty - \mathrm{i}\alpha_w A_M^{(2)}, \tag{2.22}$$

where the constants I_2, J_∞ are defined by (A 3) and (A 5) of Appendix A respectively.

In the lower deck, the appropriate transverse coordinate is

$$Y = R^{1/8} y.$$

In terms of Y, the wall position is given as

$$Y = hF_w(\mathrm{e}^{\mathrm{i}\alpha_w \bar{x}} + \text{c.c.}). \tag{2.23}$$

The solution can be written as

$$(U, V, P) = \epsilon(\lambda Y, 0, 0,) + \epsilon h(\tilde{U}_M, \epsilon^2 \tilde{V}_M, \epsilon \tilde{P}_M)\, \mathrm{e}^{\mathrm{i}\alpha_w \bar{x}} + \text{c.c.}$$

with

$$(\tilde{U}_M, \tilde{V}_M, \tilde{P}_M) = (\tilde{U}_M^{(1)}, \tilde{V}_M^{(1)}, \tilde{P}_M^{(1)}) + \epsilon(\tilde{U}_M^{(2)}, \tilde{V}_M^{(2)}, \tilde{P}_M^{(2)}) + \cdots. \tag{2.24}$$

Since $h \ll 1$, the leading-order terms satisfy the linearized boundary-layer equations

$$\mathrm{i}\alpha_w \tilde{U}_M^{(1)} + \tilde{V}_{M,Y}^{(1)} = 0, \tag{2.25}$$

$$\mathrm{i}\alpha_w Y\, \tilde{U}_M^{(1)} + \lambda \tilde{V}_M^{(1)} = -\mathrm{i}\alpha_w P_M^{(1)} + \tilde{U}_{M,YY}^{(1)}, \tag{2.26}$$

where we have used the fact that $\tilde{P}_M^{(1)} = P_M^{(1)}$. The no-slip condition on the wall is approximated, after linearization, by

$$\tilde{U}_M^{(1)}(0) = -\lambda F_w, \quad \tilde{V}_M^{(1)}(0) = 0,$$

while the matching condition with the main-deck solution is

$$\tilde{U}_M^{(1)} \to \lambda A_M^{(1)} \quad \text{as } Y \to \infty.$$

Solving these equations, we obtain

$$\tilde{U}_M^{(1)} = \lambda F_w \left\{ \frac{1}{D(\alpha_w)} \int_0^{\zeta} \mathrm{Ai}(\zeta)\, \mathrm{d}\zeta - 1 \right\}, \tag{2.27}$$

$$\bar{P}_M^{(1)} = P_M^{(1)} = \tilde{P}_M^{(1)} = -\alpha_w^{-2} (\mathrm{i}\alpha_w \lambda)^{5/3} \mathrm{Ai}'(0) F_w / D(\alpha_w), \tag{2.28}$$

where $\zeta = (\mathrm{i}\alpha_w \lambda)^{1/3} Y$, Ai is the Airy function, and

$$D(\alpha_w) = \int_0^{\infty} \mathrm{Ai}(\zeta)\, \mathrm{d}\zeta + \alpha_w^{-3} (\mathrm{i}\alpha_w \lambda)^{5/3} \mathrm{Ai}'(0). \tag{2.29}$$

The second-order correction $\tilde{U}_M^{(2)}$, $\tilde{V}_M^{(2)}$ and $\tilde{P}_M^{(2)}$ satisfy

$$\mathrm{i}\alpha_w \tilde{U}_M^{(2)} + \tilde{V}_{M,Y}^{(2)} = 0, \tag{2.30}$$

$$\mathrm{i}\alpha_w Y\, \tilde{U}_M^{(2)} + \lambda \tilde{V}_M^{(2)} = -\mathrm{i}\alpha_w \tilde{P}_M^{(2)} + \tilde{U}_{M,YY}^{(2)}. \tag{2.31}$$

It can be shown that

$$\tilde{V}_{M,\zeta}^{(2)} = C_2 \int_0^{\zeta} \mathrm{Ai}(\zeta)\, \mathrm{d}\zeta$$

with C_2 being a constant. Matching $\tilde{V}_{M,\zeta}^{(2)}$ with $V_{M,y}^{(2)}$ in the main part of the boundary layer yields

$$C_2 \int_0^{\infty} \mathrm{Ai}(\zeta)\, \mathrm{d}\zeta = -(\mathrm{i}\alpha_w \lambda)^{2/3} \left\{ A_M^{(2)} - P_M^{(1)} J_0 \right\}, \tag{2.32}$$

with J_0 defined by (A 4). The no-slip condition on the wall implies $V^{(2)}_{M,YYY}(0) = \alpha_w^2 \tilde{P}^{(2)}_M$, i.e.

$$C_2 \mathrm{Ai}'(0) = \alpha_w^2 (\mathrm{i}\alpha_w \lambda)^{-1} \tilde{P}^{(2)}_M. \tag{2.33}$$

It follows from (2.21)–(2.22) and (2.32)–(2.33) that

$$\bar{P}^{(2)}_M = -\frac{\alpha_w P^{(1)}_M}{D(\alpha_w)} \left\{ \alpha_w^{-3} (\mathrm{i}\alpha_w \lambda)^{5/3} \mathrm{Ai}'(0)(J_\infty - J_0) + I_2 \int_0^\infty \mathrm{Ai}(\zeta)\, \mathrm{d}\zeta \right\}, \tag{2.34}$$

$$\tilde{P}^{(2)}_M = -\alpha_w^{-2} (\mathrm{i}\alpha_w \lambda)^{5/3} P^{(1)}_M (J_\infty - J_0 - I_2)/D(\alpha_w), \tag{2.35}$$

$$\tilde{U}^{(2)}_M = \frac{\lambda P^{(1)}_M}{D(\alpha_w)} (J_\infty - J_0 - I_2) \int_0^\zeta \mathrm{Ai}(\zeta)\, \mathrm{d}\zeta. \tag{2.36}$$

From the x-momentum equations in (2.26) and (2.31), the vertical velocity components $\tilde{V}^{(1)}_M$ and $\tilde{V}^{(2)}_M$ are obtained as

$$\tilde{V}^{(j)}_M = \frac{1}{\lambda} \left(\tilde{U}^{(j)}_{M,YY} - \mathrm{i}\alpha_w Y \tilde{U}^{(j)}_M - \mathrm{i}\alpha_w \tilde{P}^{(j)}_M \right) \quad (j = 1, 2). \tag{2.37}$$

3. Receptivity to the vortical disturbance

3.1. *Upper deck and nonlinear interaction*

When both the roughness and the vortical disturbance are present, the expansion in the upper deck takes form

$$\begin{aligned} \boldsymbol{u} = (1, 0, 0) + \epsilon^2 h \boldsymbol{u}_M + \epsilon_c \boldsymbol{u}_c \\ + \epsilon\epsilon_c h R^{1/16} (\bar{\boldsymbol{u}}_1 + \epsilon \bar{\boldsymbol{u}}_2 + \epsilon^2 \bar{\boldsymbol{u}}_3) E + \epsilon^2 \epsilon_c h (\boldsymbol{u}_4 + \epsilon \bar{\boldsymbol{u}}_5 E) + \text{ c.c.} + \cdots, \end{aligned} \tag{3.1}$$

$$p = \epsilon^2 h \bar{p}_M \, \mathrm{e}^{\mathrm{i}\alpha_w \bar{x}} + \epsilon\epsilon_c h R^{1/16} (\bar{p}_1 + \epsilon \bar{p}_2 + \epsilon^2 \bar{p}_3) E + \epsilon^2 \epsilon_c h (p_4 + \epsilon \bar{p}_5 E) + \text{ c.c.} + \cdots, \tag{3.2}$$

where a bold letter denotes a vector, and $\boldsymbol{u}_M = (\bar{u}_M, \bar{v}_M)\, \mathrm{e}^{\mathrm{i}\alpha_w \bar{x}}$ denotes the mean-flow distortion in the upper deck as given by (2.20). For convenience, we define

$$E = \exp\{\mathrm{i}(\alpha \bar{x} + \beta \bar{z} - \omega \bar{t})\},$$

where the scaled wavenumber and frequency of the T-S wave, α and ω, expand as (Smith 1979*a*)

$$\alpha = \alpha_1 + \epsilon \alpha_2 + \epsilon^2 \alpha_3 + O(\epsilon^3 \log \epsilon), \tag{3.3}$$

$$\omega = \omega_1 + \epsilon \omega_2 + \epsilon^2 \omega_3 + O(\epsilon^3 \log \epsilon). \tag{3.4}$$

The $O(\epsilon_c)$ term in (3.1)–(3.2) represents the convecting gust. In general the gust is random in nature and must be represented as a (stochastic) Fourier integral. For simplicity, in the present study we consider the simplest situation where the gust consists of only one Fourier component, that is

$$\boldsymbol{u}_c = \bar{\boldsymbol{u}}_c(\bar{y})\, \mathrm{e}^{\mathrm{i}\alpha_c(\epsilon \bar{x} - \bar{t}) + \mathrm{i}\beta \bar{z}} + \text{c.c.}, \tag{3.5}$$

where the frequency and the spanwise wavenumber of the gust have the same scaling as those of the T-S wave respectively. Note that we allow the vertical variation of the gust to occur on the upper-deck variable, much faster than was assumed in Duck *et al.* (1996). For the specific purpose of calculating the gust/mean-flow interaction, the present scaling results in a more general setting, from which the case considered by Duck *et al.* can be recovered by taking a suitable limit (see § 3.5).

A difficulty in studying the receptivity to the vortical disturbance has been the

specification of a realistic distribution $\bar{\boldsymbol{u}}_c$. The recent experiments of Dietz (1999), in which the gust is a convecting wake produced by a vibrating ribbon in the oncoming flow, show that provided the centre of the wake is far away from the plate, the detailed structure of $\bar{\boldsymbol{u}}_c$ becomes irrelevant. As far as the receptivity is concerned, the only relevant parameter that characterizes the wake is its slip velocity, i.e. the streamwise velocity at the outer edge of the boundary layer. We shall provide mathematical evidence to support this conclusion, which is important as it will enable us to circumvent the difficulty mentioned above. Our analysis will therefore proceed independently of $\bar{\boldsymbol{u}}_c$. But as a reference, let us consider the case where the vorticity fluctuation in the far field (i.e. $\bar{y} \to \infty$) is given by

$$\Omega_\infty \exp\{\mathrm{i}\alpha_c(\epsilon\bar{x} - \bar{t}) + \mathrm{i}\beta_v\bar{y} + \mathrm{i}\beta\bar{z}\}. \tag{3.6}$$

In the $\bar{y} = O(1)$ region, $\bar{\boldsymbol{u}}_c \equiv (\bar{u}_c, \epsilon\bar{v}_c, \epsilon\bar{w}_c)$ has the solution

$$\left.\begin{aligned} \bar{u}_c &= u_\infty \mathrm{e}^{\mathrm{i}\beta_v\bar{y}} + \frac{\mathrm{i}\epsilon^2\alpha_c}{\gamma} v_\infty \mathrm{e}^{-\gamma\bar{y}}, \\ \bar{v}_c &= v_\infty(\mathrm{e}^{\mathrm{i}\beta_v\bar{y}} - \mathrm{e}^{-\gamma\bar{y}}), \\ \bar{w}_c &= w_\infty \mathrm{e}^{\mathrm{i}\beta_v\bar{y}} + \frac{\mathrm{i}\beta}{\gamma} v_\infty \mathrm{e}^{-\gamma\bar{y}}, \end{aligned}\right\} \tag{3.7}$$

where $\gamma = (\epsilon^2\alpha_c^2 + \beta^2)^{1/2}$, and $\boldsymbol{u}_\infty \equiv (u_\infty, \epsilon v_\infty, \epsilon w_\infty)$ is related to Ω_∞ by the relation

$$\boldsymbol{u}_\infty = \frac{\mathrm{i}}{|\boldsymbol{k}|^2}\boldsymbol{k} \times \Omega_\infty, \quad \boldsymbol{k} \equiv (\epsilon\alpha_c, \beta_v, \beta).$$

It follows immediately that $\boldsymbol{k} \cdot \boldsymbol{u}_\infty = 0$, i.e.

$$\alpha_c u_\infty + \beta_v v_\infty + \beta w_\infty = 0. \tag{3.8}$$

As was mentioned earlier, experimental measurements are usually carried out under the condition where the detuning is present. In order to be able to make a comprehensive comparison, we include the detuning effect in our theory by allowing $(\alpha_w + \epsilon\alpha_c)$ to have an $O(R^{-3/16})$ difference from α, that is $\alpha_w + \epsilon\alpha_c = \alpha + R^{-3/16}\alpha_d$ with $\alpha_d = O(1)$. For a gust with a given frequency ω_c and a wavy wall with the wavenumber α_w, the detuning parameter α_d is given by

$$\alpha_d \approx R^{3/16}\left[(\alpha_w + \epsilon\alpha_c) - (\alpha_1 + \epsilon\alpha_2 + \epsilon^2\alpha_3)\right]. \tag{3.9}$$

As will become clear, for a complete second-order receptivity theory, α_d must have an $O(\epsilon)$ accuracy. This is the reason why the $O(\epsilon^2)$ correction to the dispersion relation has been included in (3.9), because neglecting this higher-order term will cause an error of $O(R^{-1/16})$ in α_d.

The $O(\epsilon\epsilon_c hR^{1/16})$ terms in (3.1)–(3.2) stand for the T-S wave, and they must be included to ensure that the forced problem at the next order has an acceptable solution. For our purpose, we only need $\bar{p}_1$ and $\bar{v}_1$. They are governed by the equations

$$\frac{\partial^2\bar{p}_1}{\partial\bar{y}^2} - \{\alpha_1^2 + \beta^2\}\bar{p}_1 = 0, \quad \mathrm{i}\alpha_1\bar{v}_1 = -\frac{\partial\bar{p}_1}{\partial\bar{y}}, \tag{3.10}$$

which have the solutions

$$\bar{p}_1 = P_1 A(x_1)\mathrm{e}^{-\gamma_1\bar{y}}, \quad \bar{v}_1 = -\frac{\mathrm{i}\gamma_1}{\alpha_1}P_1 A(x_1)\mathrm{e}^{-\gamma_1\bar{y}}, \tag{3.11}$$

with $\gamma_1^2 = \alpha_1^2 + \beta^2$ and P_1 being a constant. The function $A(x_1)$ is the amplitude of the T-S wave, the determination of which is the main purpose of the present paper.

In the expansions (3.1)–(3.2), the terms with subscripts '2' and '3' represent the $O(\epsilon)$ and $O(\epsilon^2)$ corrections to the T-S wave solution respectively (which also applies to the main- and lower-deck expansions below). These can be solved to obtain α_2, ω_2, α_3 and ω_3 in (3.3)–(3.4), via a procedure that is a slight extension of that in Smith (1979*a*) to the three-dimensional T-S wave. We shall only present the calculation of the terms with subscript '2'. The details of calculating the terms with subscript '3' is of little relevance for the calculation of receptivity; so we only give the final result in Appendix A.

The governing equations for $\bar{p}_2$ and $\bar{v}_2$ in (3.1)–(3.2) are

$$\bar{p}_{2,\bar{y}\bar{y}} - (\alpha_1^2 + \beta^2)\bar{p}_2 = 2\alpha_1\alpha_2\bar{p}_1, \quad \mathrm{i}\alpha_1\bar{v}_2 + \mathrm{i}(\alpha_2 - \omega_1)\bar{v}_1 = -\bar{p}_{2,\bar{y}}. \tag{3.12}$$

We find that

$$\bar{p}_2 = \bar{P}_2\,\mathrm{e}^{-\gamma_1\bar{y}} - \frac{\alpha_1\alpha_2}{\gamma_1}AP_1\bar{y}\,\mathrm{e}^{-\gamma_1\bar{y}}, \tag{3.13}$$

where $\bar{P}_2$ is an arbitrary function of x_1. Substituting $\bar{p}_2$ into the equation for $\bar{v}_2$, we find that as $\bar{y} \to 0$

$$\bar{v}_2 \to -\frac{\mathrm{i}\gamma_1}{\alpha_1}\bar{P}_2 + \mathrm{i}\left\{\frac{(\alpha_2 - \omega_1)\gamma_1}{\alpha_1^2} - \frac{\alpha_2}{\gamma_1}\right\}AP_1. \tag{3.14}$$

We now turn to the $O(\epsilon^2\epsilon_c h)$ terms, which are driven directly by the interaction between the convecting gust and the mean-flow distortion. Substituting (3.1)–(3.2) into the Navier-Stokes equations, we obtain

$$\nabla\cdot\boldsymbol{u}_4 = -\frac{\partial u_1}{\partial x_1}E, \tag{3.15}$$

$$\frac{\partial}{\partial\bar{x}}\boldsymbol{u}_4 = -\nabla p_4 - \left\{\frac{\partial\boldsymbol{u}_1}{\partial x_1} + \frac{\partial\bar{p}_1}{\partial x_1}\mathbf{i}\right\}E - (\boldsymbol{u}_M\cdot\nabla)\boldsymbol{u}_c - (\boldsymbol{u}_c\cdot\nabla)\boldsymbol{u}_M, \tag{3.16}$$

where the operator ∇ (and ∇^2 below) are defined with respect to the scaled variables $\bar{x}$, $\bar{y}$ and $\bar{z}$. Equations (3.15)–(3.16) can be reduced to a single equation for the pressure p_4:

$$\nabla^2 p_4 = -2\mathrm{i}\alpha_1 A'(x_1)P_1\,\mathrm{e}^{-\gamma_1\bar{y}}\,E - R_p, \tag{3.17}$$

where

$$R_p = \nabla\cdot\{(\boldsymbol{u}_M\cdot\nabla)\boldsymbol{u}_c + (\boldsymbol{u}_c\cdot\nabla)\boldsymbol{u}_M\}. \tag{3.18}$$

After a straightforward calculation aided by (3.8), we find that $R_p = \bar{R}_p\,\mathrm{e}^{\mathrm{i}\alpha_d x_1}E + \text{c.c.}$ with

$$\bar{R}_p(\bar{y}) = 2\alpha_w\left(\mathrm{i}\bar{u}_c' + 2\mathrm{i}\epsilon\alpha_c\bar{u}_c + \mathrm{i}\epsilon\beta\bar{w}_c - \epsilon^2\alpha_c\bar{v}_c\right)\bar{v}_M, \tag{3.19}$$

where $\bar{v}_M = -\mathrm{i}(\bar{P}_M^{(1)} + \bar{P}_M^{(2)})\,\mathrm{e}^{-\alpha_w\bar{y}}$ with $\bar{P}_M^{(1)}$ and $\bar{P}_M^{(2)}$ given by (2.28) and (2.34) respectively. The solutions for p_4 and $\boldsymbol{u}_4$ take the form $p_4 = (\bar{p}_4E + \text{c.c.})$ and $\boldsymbol{u}_4 = (\bar{\boldsymbol{u}}_4E + \text{c.c.})$. The function $\bar{p}_4$ is found to be

$$\bar{p}_4 = \left\{P_4 + \frac{\mathrm{i}\alpha_1}{\gamma_1}A'(x_1)P_1\bar{y}\right\}\mathrm{e}^{-\gamma_1\bar{y}} - \bar{Q}_p\,\mathrm{e}^{\mathrm{i}\alpha_d x_1}, \tag{3.20}$$

where P_4 is an undetermined function of x_1 representing the complementary solution, while

$$\bar{Q}_p = \mathrm{e}^{-\gamma_1 \bar{y}} \int_0^{\bar{y}} \mathrm{e}^{2\gamma_1 \bar{y}_1} \int_\infty^{\bar{y}_1} \bar{R}_p(\bar{y}_2)\, \mathrm{e}^{-\gamma_1 \bar{y}_2}\, \mathrm{d}\bar{y}_2\, \mathrm{d}\bar{y}_1. \tag{3.21}$$

By substituting p_4 into the vertical momentum equation in (3.16), it can be shown that

$$\begin{aligned}\bar{v}_4 = (\mathrm{i}\alpha_1)^{-1} \Big\{ & -[\mathrm{i}(\alpha_w - \epsilon\alpha_c)\bar{u}_c - \mathrm{i}\epsilon\beta\bar{w}_c - \epsilon(\alpha_w - \epsilon\alpha_c)\bar{v}_c]\, \bar{v}_M\, \mathrm{e}^{\mathrm{i}\alpha_d x_1} \\ & + \left[-\frac{\mathrm{i}\alpha_1}{\gamma_1} A' P_1 + \gamma_1 P_4 + \frac{\mathrm{i}\gamma_1}{\alpha_1} A' P_1 + \mathrm{i}\alpha_1 A' P_1 \bar{y} \right] \mathrm{e}^{-\gamma_1 \bar{y}} \\ & + \left[\mathrm{e}^{\gamma_1 \bar{y}} \int_\infty^{\bar{y}} \bar{R}_p\, \mathrm{e}^{-\gamma_1 \bar{y}_1}\, \mathrm{d}\bar{y}_1 - \gamma_1 \bar{Q}_p \right] \mathrm{e}^{\mathrm{i}\alpha_d x_1} \Big\}. \end{aligned} \tag{3.22}$$

As $\bar{y} \to 0$,

$$\begin{aligned}\bar{v}_4 \to (\mathrm{i}\alpha_1)^{-1} & \left\{ F_1\, \mathrm{e}^{\mathrm{i}\alpha_d x_1} - \frac{\mathrm{i}\alpha_1}{\gamma_1} A' P_1 + \gamma_1 P_4 + \frac{\mathrm{i}\gamma_1}{\alpha_1} A' P_1 \right\} \\ & + (\mathrm{i}\alpha_1)^{-1} \left\{ \mathrm{i}\alpha_w \left[\alpha_w \bar{u}_c(0) + \bar{u}_c'(0) \right] \bar{v}_M(0)\, \mathrm{e}^{\mathrm{i}\alpha_d x_1} - \left(\gamma_1^2 P_4 - \frac{\mathrm{i}(\alpha_1^2 - \beta^2)}{\alpha_1} A' P_1 \right) \right\} \bar{y} \\ & + \cdots, \end{aligned} \tag{3.23}$$

where

$$F_1 = -\mathrm{i}\left[(\alpha_w - \epsilon\alpha_c)\bar{u}_c(0) - \epsilon\beta\bar{w}_c(0) \right] \bar{v}_M(0) - \int_0^\infty \bar{R}_p(\bar{y})\, \mathrm{e}^{-\gamma_1 \bar{y}}\, \mathrm{d}\bar{y} \tag{3.24}$$

is the forcing due to the vorticity–roughness interaction in the upper layer. It turns out that there is further forcing arising from the so-called edge layer. For the two-dimensional case, Duck *et al.* (1996) correctly included the leading-order contribution from the edge layer† by arguing that the slopes of the streamlines in the upper and main decks are the same (to leading order). But it seems impossible to use that argument to obtain the higher-order contribution. In the next subsection, we shall consider the interaction in the edge layer in some detail.

The pressure $\bar{p}_5$ in (3.2) satisfies

$$\bar{p}_{5,\bar{y}\bar{y}} - (\alpha_1^2 + \beta^2)\bar{p}_5 = 2\alpha_1\alpha_2\bar{p}_4 - 2\mathrm{i}\alpha_1\bar{p}_{2,x_1} - 2\mathrm{i}\alpha_2\bar{p}_{1,x_1}, \tag{3.25}$$

and has the solution

$$\begin{aligned}\bar{p}_5 = \left\{ \bar{P}_5 + (\mathrm{i}\beta^2\alpha_2 A' P_1 + \mathrm{i}\alpha_1\gamma_1^2\bar{P}_{2,x_1} - \alpha_1\alpha_2\gamma_1^2 P_4)\gamma_1^{-3}\bar{y} - \mathrm{i}\alpha_1^2\alpha_2\gamma_1^{-2} A' P_1 \bar{y}^2 \right\} \mathrm{e}^{-\gamma_1 \bar{y}} \\ -2\alpha_1\alpha_2 \left\{ \mathrm{e}^{-\gamma_1 \bar{y}} \int_0^{\bar{y}} \mathrm{e}^{2\gamma_1 \bar{y}_1} \int_\infty^{\bar{y}_1} \bar{Q}_p(\bar{y}_2)\, \mathrm{e}^{-\gamma_1 \bar{y}_2}\, \mathrm{d}\bar{y}_2 \mathrm{d}\bar{y}_1 \right\} \mathrm{e}^{\mathrm{i}\alpha_d x_1}. \end{aligned} \tag{3.26}$$

The solution for the velocity $\bar{v}_5$ may be found from

$$\mathrm{i}\alpha_1\bar{v}_5 + \mathrm{i}(\alpha_2 - \omega_1)\bar{v}_4 + \bar{v}_{2,x_1} = -\bar{p}_{5,\bar{y}}. \tag{3.27}$$

By substituting in (3.14), (3.22) and (3.26), it can be shown that as $\bar{y} \to 0$

$$\begin{aligned}\bar{v}_5 \to \Gamma - \left\{ \frac{\mathrm{i}(\alpha_2 - \omega_1)}{\alpha_1^2} \left(\mathrm{i}\alpha_w \bar{u}_c(0)\bar{v}_M(0) + \int_0^\infty \bar{R}_p\, \mathrm{e}^{-\gamma_1 \bar{y}}\, \mathrm{d}\bar{y} \right) + \frac{\mathrm{i}\alpha_2}{\gamma_1} \int_0^\infty \bar{y}\bar{R}_p\, \mathrm{e}^{-\gamma_1 \bar{y}}\, \mathrm{d}\bar{y} \right\} \mathrm{e}^{\mathrm{i}\alpha_d x_1} \\ + \cdots, \end{aligned} \tag{3.28}$$

† During the review process of the present paper, the author noted that Ruban, Duck & Zhikharev (1996) included this leading-order contribution by analysing the edge layer.

where Γ is defined by

$$\Gamma = -\mathrm{i}\frac{\gamma_1}{\alpha_1}\bar{P}_5 + \mathrm{i}\alpha_1^{-1}\gamma_1^{-3}(\mathrm{i}\beta^2\alpha_2 A' P_1 + \mathrm{i}\alpha_1\gamma_1^2\bar{P}_{2,x_1} - \alpha_1\alpha_2\gamma_1^2 P_4) + \gamma_1\alpha_1^{-2}\bar{P}_{2,x_1}$$
$$+\mathrm{i}\gamma_1\alpha_1^{-2}(\alpha_2-\omega_1)P_4 + \alpha_1^{-3}\gamma_1^{-1}[\alpha_1^2\alpha_2 - (\alpha_2-\omega_1)(\alpha_1^2+2\beta^2)]A' P_1. \quad (3.29)$$

In contrast to the standard triple-deck, the vertical velocities $\bar{v}_4$ and $\bar{v}_5$ in the upper deck do not match directly with those in the main deck because of the edge layer between them.

3.2. *Analysis of the edge-layer interaction*

As was first pointed out by Gulyaev *et al.* (1989), a vortical disturbance is largely 'absorbed' by a relatively thin edge layer, which sits on the outer reach of the boundary layer (see figure 1). The Blasius boundary profile there has the approximation

$$U_B \sim 1 - \frac{\hat{a}}{\hat{y}-\hat{b}}\,\mathrm{e}^{-(\hat{y}-\hat{b})^2/4},$$

where $\hat{y} = y/x^{1/2}$ is the Blasius similarity variable, $\hat{a} \approx 0.46$ and $\hat{b} \approx 1.72$. The edge layer is centred at $y = (\hat{y}_0 + \hat{b})x^{1/2} \gg 1$ and has the width $\delta = 2/\hat{y}_0 \ll 1$, where $\hat{y}_0$ is determined by

$$\hat{y}_0^3\,\mathrm{e}^{\hat{y}_0^2/4} = 4\hat{a}R^{1/4}, \quad \text{so that } \hat{y}_0 \approx (\log R)^{1/2}.$$

The local transverse variable is defined by

$$\hat{\eta} = (\hat{y} - \hat{y}_b)/\delta \quad \text{with } \hat{y}_b = \hat{y}_0 + \hat{b},$$

and thus $\hat{\eta}$ is related to the upper-deck variable $\bar{y}$ via

$$\bar{y} = \epsilon y = \epsilon x^{1/2}(\hat{y}_b + \delta\hat{\eta}). \quad (3.30)$$

We now show that the vortical disturbance, while undergoing rapid reduction within the edge layer, interacts with the mean-flow distortion, to make a contribution comparable with that from the upper deck to the receptivity.

The flow in this region has the expansion

$$u = [1 - \epsilon^2\delta^{-2}\,\mathrm{e}^{-\hat{\eta}} + \cdots] + \epsilon_c[\hat{u}_c(\hat{\eta}) + \epsilon\delta\hat{u}_c^{(1)}(\hat{\eta}) + \cdots]\,\mathrm{e}^{\mathrm{i}\epsilon\alpha_c(\bar{x}-\bar{t})+\mathrm{i}\beta\bar{z}} + \epsilon^2 h[\bar{u}_M(0) + \cdots]\,\mathrm{e}^{\mathrm{i}\alpha_w\bar{x}}$$
$$+\epsilon\epsilon_c hR^{1/16}[A(x_1)\bar{u}_1(0) + \cdots]E + \epsilon\delta^{-1}\epsilon_c h[\hat{u}_4 + \epsilon\hat{u}_5 + \cdots]E + \text{c.c.} + \cdots,$$

$$v = \epsilon^2\epsilon_c\delta\,[\hat{v}_c(\hat{\eta}) + \epsilon\delta\hat{v}_c^{(1)}(\hat{\eta}) + \cdots]\,\mathrm{e}^{\mathrm{i}\epsilon\alpha_c(\bar{x}-\bar{t})+\mathrm{i}\beta\bar{z}}$$
$$+\epsilon^2 h[\bar{v}_M + \epsilon\hat{y}_b x^{1/2}(-\alpha_w\bar{v}_M(0)) + \epsilon\delta(-\alpha_w\bar{v}_M(0))x^{1/2}\hat{\eta} + \cdots]\,\mathrm{e}^{\mathrm{i}\alpha_w\bar{x}}$$
$$+\epsilon\epsilon_c hR^{1/16}[A(x_1)\bar{v}_1(0) + \cdots]E + \epsilon^2\epsilon_c h[\hat{v}_4 + \epsilon\hat{v}_5 + \cdots]E + \text{c.c.} + \cdots,$$

$$w = \epsilon_c\delta\,[\hat{w}_c(\hat{\eta}) + \epsilon\delta\hat{u}_c^{(1)}(\hat{\eta}) + \cdots]\,\mathrm{e}^{\mathrm{i}\epsilon\alpha_c(\bar{x}-\bar{t})+\mathrm{i}\beta\bar{z}} + \epsilon\epsilon_c hR^{1/16}[A(x_1)\bar{w}_1(0) + \cdots]E$$
$$+\epsilon\delta^{-1}\epsilon_c h[\hat{w}_4 + \epsilon\hat{w}_5 + \cdots]E + \text{c.c.} + \cdots,$$

$$p = \epsilon^2 h[\bar{p}_M(0) + \cdots]\,\mathrm{e}^{\mathrm{i}\alpha_w\bar{x}} + \epsilon\epsilon_c hR^{1/16}[A(x_1)P_1 + \bar{P}_2 + \cdots]E$$
$$+\epsilon^2\epsilon_c h[P_4 + \bar{P}_5 + \cdots]E + \text{c.c.} + \cdots,$$

where the terms representing the mean-flow distortion and the T-S wave are just the Taylor expansions of the corresponding upper-deck solutions. The solution for the gust was first considered by Gulyaev *et al.* (1989), and was developed in more

detail by Duck *et al.* (1996) for the two-dimensional case and by Leib, Wundrow & Goldstein (1999) for the three-dimensional case. The leading-order terms, $\hat{u}_c$, $\hat{v}_c$ and $\hat{w}_c$, satisfy†

$$\left.\begin{aligned} &\mathrm{i}\alpha_c\hat{u}_c + x^{-1/2}\hat{v}_c'(\hat{\eta}) + \mathrm{i}\beta\hat{w}_c = 0,\\ &\hat{u}_c''(\hat{\eta}) + \hat{u}' + \mathrm{e}^{-\hat{\eta}}(\mathrm{i}\alpha_c x\hat{u}_c - x^{1/2}\hat{v}_c) = 0,\\ &\hat{w}_c''(\hat{\eta}) + \hat{w}_c' + (\mathrm{i}\alpha_c x)\,\mathrm{e}^{-\hat{\eta}}\,\hat{w}_c = 0, \end{aligned}\right\} \tag{3.31}$$

subject to the matching conditions with the slip velocities of the gust at the edge of the boundary layer, namely

$$\hat{u}_c \to \left[\bar{u}_c(0) + \epsilon\hat{y}_b x^{1/2}\bar{u}_c'(0)\right], \quad \hat{w}_c \to \left[\bar{w}_c(0) + \epsilon\hat{y}_b x^{1/2}\bar{w}_c'(0)\right] \text{ as } \hat{\eta}\to\infty.$$

As was pointed out by Gulyaev *et al.* (1989), the $\hat{u}_c'$ and $\hat{w}_c'$ terms in their respective equations are associated with the expanding of the boundary layer. Thus in the edge layer the non-parallelism is a leading-order effect. This implies that the use of the O-S equation to calculate the signature of the gust is not completely justified.

The relevant solution for $\hat{w}_c$ is given by Leib *et al.* (1999):

$$\hat{w}_c = \pi\mathrm{i}[\bar{w}_c(0) + \epsilon\hat{y}_b x^{1/2}\bar{w}_c'(0)](\mathrm{i}\alpha_c x)^{1/2}\,\mathrm{e}^{-\hat{\eta}/2}\,H_1^{(1)}(\hat{\zeta}), \tag{3.32}$$

where $H_1^{(1)}$ is the first-order Hankel function in the usual notation, and

$$\hat{\zeta} = 2(\mathrm{i}\alpha_c x)^{1/2}\,\mathrm{e}^{-\hat{\eta}/2}.$$

Eliminating $\hat{u}_c$ and $\hat{w}_c$ between the equations in (3.31) yields

$$\hat{v}_c''' + \hat{v}_c'' + \mathrm{i}\alpha_c x\,\mathrm{e}^{-\hat{\eta}}(\hat{v}_c' + \hat{v}_c) = 0.$$

The appropriate solution is (cf. Duck *et al.* 1996)

$$\hat{v}_c = -2\pi\{\alpha_c\bar{u}_c(0) + \beta\bar{w}_c(0) + \epsilon\hat{y}_b x^{1/2}[\alpha_c\bar{u}_c'(0) + \beta\bar{w}_c'(0)]\}x^{1/2}\hat{\zeta}^2\int_\infty^{\hat{\zeta}}\hat{\zeta}^{-3}H_0^{(1)}(\hat{\zeta})\,\mathrm{d}\hat{\zeta}, \tag{3.33}$$

where $H_0^{(1)}$ denotes the Hankel function of order zero. The exact solutions for $\hat{u}_c^{(1)}$, $\hat{v}_c^{(1)}$ and $\hat{w}_c^{(1)}$ are not needed; all that we require is that

$$\hat{u}_c^{(1)} \to \bar{u}_c'(0)x^{1/2}\hat{\eta} \quad \text{as } \hat{\eta}\to\infty, \quad \text{and} \quad \hat{u}_c^{(1)} \to 0 \quad \text{as } \hat{\eta}\to-\infty.$$

The edge-layer solutions (3.32) and (3.33) are valid for arbitrary x. But in the following analysis of the gust–roughness interaction, x will be assigned the value $x_0 = 1$.

The terms with the subscripts '4' and '5' in the expansion are directly driven by the vorticity–roughness interaction. Strictly speaking, $(\hat{u}_5, \hat{v}_5, \hat{w}_5)$ should expand as power series of δ, i.e. $\hat{u}_5 = \delta^{-1}\hat{u}_5^{(1)} + \hat{u}_5^{(2)} + \delta\hat{u}_5^{(3)} + \cdots$ etc. However, such a formal procedure can be avoided by tactically retaining the $O(\epsilon\delta^{-1})$ forcing terms in the equation for $(\hat{u}_4, \hat{v}_4)$, and the $O(\delta)$ terms in the equations for $(\hat{u}_5, \hat{v}_5, \hat{w}_5)$. This leads to

$$\mathrm{i}\alpha_1\hat{u}_4 + \hat{v}_{4,\hat{\eta}} = 0, \quad \mathrm{i}\alpha_1\hat{u}_4 = -(1 - \epsilon\hat{y}_b\alpha_w)\bar{v}_M(0)\hat{u}_c'(\hat{\eta}), \quad \hat{w}_4 \equiv 0; \tag{3.34}$$

$$\mathrm{i}\alpha_1\hat{u}_5 + \hat{v}_{5,\hat{\eta}} + \mathrm{i}\beta\hat{w}_5 = -\delta A'\bar{u}_1(0) - \mathrm{i}\alpha_2\hat{u}_4,$$

† Note that the two-dimensional version of the equations is the same as that for the so-called Brown–Stewartson (1973) eigensolution, but the latter solution matches to an outer solution which is viscous in nature.

$$\mathrm{i}\alpha_1\hat{u}_5 + \mathrm{i}(\alpha_2-\omega_1)\hat{u}_4 = -\delta[\mathrm{i}\alpha_1\bar{P}_4 + A'P_1 + A'\bar{u}_1(0)] - \delta\bar{v}_M(0)\hat{u}^{(1)}_{c,\hat{\eta}},$$
$$-\delta[\mathrm{i}\alpha_w\bar{u}_M(0)\hat{u}_c(\hat{\eta}) - \alpha_w\bar{v}_M(0)\hat{\eta}\hat{u}'_c(\hat{\eta})],$$
$$\mathrm{i}\alpha_1\hat{w}_5 = -\delta[\mathrm{i}\beta\bar{P}_4 + A'\bar{w}_1(0)] - \bar{v}_M(0)\hat{w}'_c(\hat{\eta}).$$

These equations can be solved to give

$$\hat{v}_4 = C_4 + (1-\epsilon\hat{y}_b\alpha_w)\bar{v}_M(0)\hat{u}_c(\hat{\eta}), \tag{3.35}$$

$$\hat{v}_5 = C_5 + \frac{\omega_1}{\alpha_1}(1-\epsilon\hat{y}_b\alpha_w)\bar{v}_M(0)\hat{u}_c(\hat{\eta}) + \delta\left[\frac{\mathrm{i}\gamma_1^2}{\alpha_1}\bar{P}_4 + (1-\frac{\beta^2}{\alpha_1^2})A'P_1\right]\hat{\eta} + \frac{\beta}{\alpha_1}\bar{v}_M(0)\hat{w}_c(\hat{\eta})$$
$$-\delta\alpha_w\bar{v}_M(0)\left[\hat{\eta}\hat{u}_c(\hat{\eta}) - 2\int_{-\infty}^{\hat{\eta}}\hat{u}_c(\hat{\eta})\mathrm{d}\hat{\eta}\right] + \delta\bar{v}_M(0)\hat{u}^{(1)}_c(\hat{\eta}) \tag{3.36}$$

where C_4 and C_5 are functions of x_1, to be found by matching with the upper-deck solution. It is straightforward to write down the asymptote of the edge-layer solution $(\hat{v}_4 + \epsilon\hat{v}_5)$ as $\hat{\eta}\to\infty$. On re-writing it in terms of $\bar{y}$ (see (3.30)) and matching with the upper-deck solution (3.23) and (3.28), we find that

$$C_4 = (\mathrm{i}\alpha_1)^{-1}\left\{F_1\,\mathrm{e}^{\mathrm{i}\alpha_d x_1} + \left[-\frac{\mathrm{i}\hat{\alpha}_1}{\hat{\gamma}_1}A'P_1 + \gamma_1 P_4 + \frac{\mathrm{i}\gamma_1}{\alpha_1}A'P_1\right]\right\}$$
$$+\left\{-\left[\bar{u}_c(0) + \epsilon\frac{\beta}{\alpha_1}\bar{w}_c(0)\right]\bar{v}_M(0) + 2\epsilon\hat{y}_b\alpha_w\bar{u}_c(0)\bar{v}_M(0)\right\}\mathrm{e}^{\mathrm{i}\alpha_d x_1},$$

$$C_5 = \Gamma + \left\{\frac{\mathrm{i}\gamma_1^2}{\alpha_1}P_4 + \left(1-\frac{\beta^2}{\alpha_1^2}\right)A'P_1\right\}\hat{y}_b - \frac{\omega_1}{\alpha_1}\bar{v}_M(0)\bar{u}_c(0) - 2\delta\alpha_w\bar{v}_M(0)J_c,$$
$$-\left\{\frac{\mathrm{i}(\alpha_2-\omega_1)}{\alpha_1^2}\left(\mathrm{i}\alpha_w\bar{u}_c(0)\bar{v}_M(0) + \int_0^\infty\bar{R}_p\,\mathrm{e}^{-\gamma_1\bar{y}}\,\mathrm{d}\bar{y}\right) + \frac{\mathrm{i}\alpha_2}{\gamma_1}\int_0^\infty\bar{y}\bar{R}_p\,\mathrm{e}^{-\gamma_1\bar{y}}\,\mathrm{d}\bar{y}\right\}\mathrm{e}^{\mathrm{i}\alpha_d x_1},$$

where

$$J_c = -\left[(\bar{u}_c(0) + \frac{\beta}{\alpha_c}\bar{w}_c(0)) + \left(2\gamma_E + \log\alpha_c - \tfrac{1}{2}\pi\mathrm{i}\right)\bar{u}_c(0)\right]$$

with $\gamma_E \approx 0.5772$ being Euler's constant.

3.3. *The main-deck solution*

In the main part of the boundary layer, where $y = O(1)$, the solution expands as

$$u = U_B + \epsilon hU_M + \epsilon_c hR^{1/16}[AU_1 + \epsilon U_2 + \epsilon^2 U_3]E + \epsilon\epsilon_c h(U_4 + \epsilon U_5)E + \cdots, \tag{3.37}$$

$$v = \epsilon^2 hV_M + \epsilon\epsilon_c hR^{1/16}[AV_1 + \epsilon V_2 + \epsilon^2 V_3]E + \epsilon^2\epsilon_c h(V_4 + \epsilon V_5)E + \cdots, \tag{3.38}$$

$$w = \epsilon_c hR^{1/16}[AW_1 + \epsilon W_2 + \epsilon^2 W_3]E + \epsilon\epsilon_c h(W_4 + \epsilon W_5)E + \cdots, \tag{3.39}$$

$$p = \epsilon^2 hP_M + \epsilon\epsilon_c hR^{1/16}[AP_1 + \epsilon P_2 + \epsilon^2 P_3]E + \epsilon^2\epsilon_c h(P_4 + \epsilon P_5)E + \cdots. \tag{3.40}$$

Since no further interaction takes place there, the components on the T-S wave scales arise merely as the response to the forcing from the upper and edge layers, and are governed by the standard main-deck equations. Here instead of expanding U_B about x_0, it is more convenient to work out the main-deck solutions for an arbitrary x first, and subsequently expand their large- and small-y asymptotes before matching with the upper- and lower-deck solutions. The leading-order streamwise and vertical velocities of the T-S wave have the familiar solution

$$U_1 = B_1U'_B, \quad V_1 = -\mathrm{i}\alpha_1 B_1 U_B, \quad W_1 = 0, \tag{3.41}$$

where B_1 is a constant and is related to P_1 via

$$\alpha_1^2 B_1 = \gamma_1 P_1, \tag{3.42}$$

a relation provided by matching (3.41) to the upper-deck solution (3.11).

The terms U_2, V_2 etc. stand for the $O(R^{-1/8})$ correction to the T-S wave solution, and they satisfy

$$\mathrm{i}\alpha_1 U_2 + V_{2,y} + \mathrm{i}\beta W_2 = -\mathrm{i}\alpha_2 A U_1, \tag{3.43}$$

$$\mathrm{i}\alpha_1 U_B U_2 + U_B' V_2 = -\mathrm{i}(\alpha_2 U_B - \omega_1) A U_1 - \mathrm{i}\alpha_1 A P_1, \tag{3.44}$$

$$\mathrm{i}\alpha_1 U_B W_2 = -\mathrm{i}\beta A P_1, \qquad \mathrm{i}\alpha_1 A U_B V_1 = -P_{2,y}. \tag{3.45}$$

They are solved, after inserting in (3.41), to give (cf. Ryzhov & Terent'ev 1977; Smith 1979*a*)

$$V_2 = -\mathrm{i}\alpha_1 B_2 U_B + \mathrm{i}\omega_1 A B_1 + \mathrm{i}\gamma_1^2 \alpha_1^{-1} A P_1 U_B \int^y \frac{\mathrm{d}y}{U_B^2}, \tag{3.46}$$

$$P_2 = \tilde{P}_2 - \alpha_1^2 A B_1 \int_0^y U_B^2 \mathrm{d}y, \tag{3.47}$$

where B_2 and $\tilde{P}_2$ are functions of x_1 to be determined later. It is easy to show that as $y \to \infty$

$$\left.\begin{aligned} V_2 &\to (\mathrm{i}\gamma_1^2 \alpha_1^{-1} A P_1) y + \left(-\mathrm{i}\alpha_1 B_2 U_B + \mathrm{i}\omega_1 A B_1 + \mathrm{i}\gamma_1^2 \alpha_1^{-1} A P_1 J_\infty(x)\right) + \cdots, \\ P_2 &\to (-\alpha_1^2 A B_1) y + \left(\tilde{P}_2 - \alpha_1^2 A B_1 I_2(x)\right) + \cdots, \end{aligned}\right\} \tag{3.48}$$

where $J_\infty(x)$ and $I_2(x)$ are given by (A 5) and (A 3) respectively.

The governing equations for U_4 and V_4 are

$$\mathrm{i}\alpha_1 U_4 + V_{4,y} = -A' U_1, \quad \mathrm{i}\alpha_1 U_B + U_B' V_4 = -A' U_B' U_1,$$

while at the next order, the functions V_5 and P_5 satisfy

$$U_B V_{5,y} - U_B' V_5 = \left(1 - \frac{\beta^2}{\alpha_1^2}\right) A' P_0 + \mathrm{i}\gamma_1^2 \alpha_1^{-1} P_4 - \mathrm{i}\omega_1 U_4, \tag{3.49}$$

$$U_B(\mathrm{i}\alpha_1 V_4 + A' V_1) = -P_{5,y}. \tag{3.50}$$

These equations can be solved in sequence to give

$$U_4 = B_4 U_B', \quad V_4 = -(A' B_1 + \mathrm{i}\alpha_1 B_4) U_B, \quad W_4 = 0; \tag{3.51}$$

$$V_5 = -\mathrm{i}\alpha_1 B_5 U_B + \mathrm{i}\omega_1 B_4 + \left\{\left(1 - \frac{\beta^2}{\alpha_1^2}\right) P_1 A' + \mathrm{i}\gamma_1^2 \alpha_1^{-1} P_4\right\} U_B \int^y \frac{\mathrm{d}y}{U_B^2}, \tag{3.52}$$

$$P_5 = \tilde{P}_5 - (\alpha_1^2 B_4 - 2\mathrm{i}\alpha_1 A' B_1) \int_0^y U_B^2 \mathrm{d}y, \tag{3.53}$$

where B_4, B_5 and $\tilde{P}_5$ are unknown functions of x_1. The large-y asymptotes of the main-deck solutions depend on x through the integrals $I_2(x)$ and $J_\infty(x)$ (see e.g. (3.48)), while their small-y asymptotes depend on x via the wall shear $\lambda(x)$. Before carrying out the matching, it is necessary to expand these asymptotes about x_0 by using (A 6) and (2.9), and rewrite the resulting expression in terms of x_1 and re-order. For brevity, we shall omit the details of these expansions, but merely illustrate this by considering the asymptote of P_2 as given in (3.48). It can be rewritten as

$$P_2 \to (-\alpha_1^2 A B_1) y + (\tilde{P}_2 - \alpha_1^2 A B_1 I_2(0)) + R^{-3/16}\{\tfrac{1}{2}\alpha_1^2 A B_1 I_2(0) x_1\} + \cdots.$$

The $O(R^{-3/16})$ term proportional to x_1 will affect the matching of the terms which are smaller by $O(R^{-3/16})$, i.e. the terms with the subscript '5'. Hereafter, I_2, J_∞ and J_0 are all evaluated at x_0 unless stated otherwise.

Now since there is no pressure variation across the edge layer, the pressure in the main deck actually matches directly with that in the upper deck, leading to

$$\bar{P}_2 = \tilde{P}_2 - \alpha_1^2 A B_1 I_2, \tag{3.54}$$

$$\bar{P}_5 = \tilde{P}_5 - (\alpha_1^2 B_4 - 2\mathrm{i}\alpha_1 A' B_1) I_2 - \tfrac{1}{2}\alpha_1^2 A B_1 I_2 x_1. \tag{3.55}$$

The vertical velocity at $O(\epsilon^2\epsilon_c h R^{1/16})$ is unaffected by the presence of the edge layer and thus matches with its upper-deck counterpart,

$$-\mathrm{i}\alpha_1 B_2 + \mathrm{i}\omega_1 A B_1 + \frac{\mathrm{i}\gamma_1^2}{\alpha_1} A P_1 J_\infty = -\frac{\mathrm{i}\gamma_1}{\alpha_1}\bar{P}_2 + \mathrm{i}\left\{\frac{(\alpha_2-\omega_1)\gamma_1}{\alpha_1^2} - \frac{\alpha_2}{\gamma_1}\right\} A P_1. \tag{3.56}$$

Matching the vertical velocity at $O(\epsilon^2\epsilon_c h)$ and $O(\epsilon^3\epsilon_c h)$ with the edge-layer solution gives

$$\alpha_1^2 B_4 - 2\mathrm{i}\alpha_1 A'(x_1) B_1 = \gamma_1 P_4 - \frac{\mathrm{i}\alpha_1}{\gamma_1} A'(x_1) P_1 + F_v\,\mathrm{e}^{\mathrm{i}\alpha_d x_1}, \tag{3.57}$$

$$-\mathrm{i}\alpha_1 B_5 + \mathrm{i}\omega_1 B_4 + \left\{\left(1 - \frac{\beta^2}{\alpha_1^2}\right) P_1 A' + \mathrm{i}\gamma_1^2\alpha_1^{-1} P_4\right\} J_\infty + \tfrac{1}{2}\mathrm{i}\gamma_1^2\alpha_1^{-1} A P_1 J_\infty x_1 = \Gamma + (\mathrm{i}\alpha_1)^{-1} F_c\,\mathrm{e}^{\mathrm{i}\alpha_d x_1}, \tag{3.58}$$

where

$$F_v = -\mathrm{i}[(\alpha_w - \epsilon\alpha_c)\bar{u}_c(0) - \epsilon\beta\bar{w}_c(0)]\bar{v}_M(0) - \int_0^\infty \bar{R}_p(\bar{y})\,\mathrm{e}^{-\gamma_1\bar{y}}\,\mathrm{d}\bar{y} - \mathrm{i}[\alpha_1\bar{u}_c(0) + \epsilon\beta\bar{w}_c(0)]\bar{v}_M(0) + \epsilon\hat{y}_b(2\mathrm{i}\alpha_1\alpha_w)\bar{v}_M(0)\bar{u}_c(0) \tag{3.59}$$

is the main forcing that leads to the generation of the T-S wave, and

$$F_c = -\mathrm{i}\omega_1\bar{v}_M(0)\bar{u}_c(0) - 2\mathrm{i}\delta\alpha_1\alpha_w\bar{v}_M(0)J_c + \frac{(\alpha_2-\omega_1)}{\alpha_1}\left\{\mathrm{i}\alpha_w\bar{v}_M(0)\bar{u}_c(0) + \int_0^\infty \bar{R}_p\,\mathrm{e}^{-\gamma_1\bar{y}}\,\mathrm{d}\bar{y}\right\} + \frac{\alpha_1\alpha_2}{\gamma_1}\int_0^\infty \bar{y}\bar{R}_p\,\mathrm{e}^{-\gamma_1\bar{y}}\,\mathrm{d}\bar{y}. \tag{3.60}$$

For later reference, we perform integration by parts in the integral in (3.59) to obtain

$$\int_0^\infty \bar{R}_p(\bar{y})\,\mathrm{e}^{-\gamma_1\bar{y}}\,\mathrm{d}\bar{y} = \frac{2\mathrm{i}\alpha_w\bar{v}_M(0)}{\alpha_w+\gamma_1}\left\{\epsilon[2\alpha_c\bar{u}_c(0) + \beta\bar{w}_c(0)] + \int_0^\infty [(\alpha_w+\gamma_1)\bar{u}_c' + \epsilon(2\alpha_c\bar{u}_c' + \beta\bar{w}_c')]\,\mathrm{e}^{-(\alpha_w+\gamma_1)\bar{y}}\,\mathrm{d}\bar{y}\right\} + O(\epsilon^2), \tag{3.61}$$

where the $O(\epsilon^2)$ term in the integrand has been legitimately neglected.

3.4. *The lower-deck response*

In the lower deck, where $Y = R^{1/8}y = O(1)$, the mean flow is approximated, to the required order, by $R^{-1/8}\lambda Y$, with the skin friction λ given by (2.9). The solution expands as

$$u = \epsilon(\lambda_0 + R^{-3/16}\lambda_1 x_1)Y + \epsilon h\tilde{U}_M\,\mathrm{e}^{\mathrm{i}\alpha_w\bar{x}} + \epsilon_c h R^{1/16}[A(x_1)\tilde{U}_1 + \epsilon\tilde{U}_2 + \epsilon^2\tilde{U}_3]E + \epsilon\epsilon_c h(\tilde{U}_4 + \epsilon\tilde{U}_5)E + \text{c.c.} + \cdots, \tag{3.62}$$

$$v = \epsilon^3 h\tilde{V}_M\,\mathrm{e}^{\mathrm{i}\alpha_w\bar{x}} + \epsilon^2\epsilon_c h R^{1/16}[A(x_1)\tilde{V}_1 + \epsilon\tilde{V}_2 + \epsilon^2\tilde{V}_3]E + \epsilon^3\epsilon_c h(\tilde{V}_4 + \epsilon\tilde{V}_5)E + \text{c.c.} + \cdots, \quad (3.63)$$

$$w = \epsilon_c h R^{1/16}[A(x_1)\tilde{W}_1 + \epsilon\tilde{W}_2 + \epsilon^2\tilde{W}_3]E + \epsilon\epsilon_c h(\tilde{W}_4 + \epsilon\tilde{W}_5)E + \text{c.c.} + \cdots, \quad (3.64)$$

$$p = \epsilon^2 h\tilde{P}_M\,\mathrm{e}^{\mathrm{i}\alpha_w\bar{x}} + \epsilon\epsilon_c h R^{1/16}[A(x_1)P_1 + \epsilon\tilde{P}_2 + \epsilon^2\tilde{P}_3]E + \epsilon^2\epsilon_c h(P_4 + \epsilon\tilde{P}_5)E + \cdots. \quad (3.65)$$

Here we have ignored the exponentially small signature of the convecting gust, as well as the unsteady components which are not in resonance with the T-S wave. The leading-order T-S wave solution satisfies the linearized boundary-layer equations

$$\mathrm{i}\alpha_1\tilde{U}_1 + \tilde{V}_{1,Y} + \mathrm{i}\beta\tilde{W}_1 = 0, \quad (3.66)$$

$$\mathrm{i}(\alpha_1\lambda_0 Y - \omega_1)\tilde{U}_1 + \lambda_0\tilde{V}_1 = -\mathrm{i}\alpha_1 P_1 + \tilde{U}_{1,YY}, \quad (3.67)$$

$$\mathrm{i}(\alpha_1\lambda_0 Y - \omega_1)\tilde{W}_1 = -\mathrm{i}\beta P_1 + \tilde{W}_{1,YY}. \quad (3.68)$$

The above system is subject to the matching condition with the main deck:

$$\tilde{V}_{1,Y} \to -\mathrm{i}\alpha_1\lambda_0 B_1, \quad \tilde{W}_1 \to 0 \quad \text{as } Y \to \infty, \quad (3.69)$$

and the no-slip condition $\tilde{U}_1 = \tilde{V}_1 = \tilde{W}_1 = 0$ on the wall ($Y = 0$); the latter leads to

$$\tilde{V}_{1,YYY}(0) = (\alpha_1^2 + \beta^2)P_1 \quad (3.70)$$

after setting $Y = 0$ in (3.67)–(3.68) and using (3.66).

By eliminating the pressure from (3.66)–(3.68), it can be shown that $\tilde{V}_{1,YY}$ satisfies

$$\left\{\frac{\partial^2}{\partial Y^2} - \mathrm{i}(\alpha_1\lambda_0 Y - \omega_1)\right\}\tilde{V}_{1,YY} = 0, \quad (3.71)$$

which has the solution

$$\tilde{V}_{1,Y} = \int_{\eta_0}^{\eta} \mathrm{Ai}(\eta)\mathrm{d}\eta, \quad (3.72)$$

where Ai denotes the Airy function, and

$$\eta = (\mathrm{i}\alpha_1\lambda_0)^{1/3}Y + \eta_0, \quad \eta_0 = -\mathrm{i}\omega_1(\mathrm{i}\alpha_1\lambda_0)^{-2/3}. \quad (3.73)$$

Application of (3.69) and (3.70) together with (3.73) gives

$$\int_{\eta_0}^{\infty} \mathrm{Ai}(\eta)\mathrm{d}\eta = -\mathrm{i}\alpha_1\lambda_0 B_1, \quad (\mathrm{i}\alpha_1\lambda_0)^{2/3}\mathrm{Ai}'(\eta_0) = (\alpha_1^2 + \beta^2)P_1, \quad (3.74)$$

which with (3.42) leads to the dispersion relation (Lin 1946; Smith 1979*a*)

$$\Delta(\lambda_0) \equiv \mathrm{i}\alpha_1\int_{\eta_0}^{\infty} \mathrm{Ai}(\eta)\mathrm{d}\eta - \lambda_0[\alpha_1^2 + \beta^2]^{-1/2}(\mathrm{i}\alpha_1\lambda_0)^{2/3}\mathrm{Ai}'(\eta_0) = 0. \quad (3.75)$$

We are only interested in the neutral modes, for which the wavenumbers α_1 and β, and frequency ω_1 are all real, and are determined by

$$\alpha_1 = \lambda_0^{5/4}\alpha_N, \quad \beta = \lambda_0^{5/4}\beta_N, \quad \omega_1 = \lambda_0^{3/2}\omega_N,$$

with α_N, β_N and ω_N being given by

$$\alpha_N^{1/3} = d_1\left(\alpha_N^2 + \beta_N^2\right)^{-1/2}, \quad \omega_N = d_2\alpha_N^{2/3},$$

where $d_1 \approx 1.009$ and $d_2 \approx 2.29$; for details see Smith (1979*a*).

For later reference, we give the solution of the leading-order spanwise velocity

$$\tilde{W}_1 = \frac{\mathrm{i}\beta \mathrm{Ai}'(\eta_0)}{\alpha_1^2+\beta^2}Ł(\eta), \tag{3.76}$$

where $Ł(\eta)$ is the solution to the equation

$$Ł'' - \eta Ł = 1 \tag{3.77}$$

subject to the boundary condition $Ł(\eta_0) = 0$ and $Ł(\infty) = 0$. It follows from (3.66), (3.72) and (3.76) that the leading-order streamwise velocity of the T-S wave

$$\tilde{U}_1 = -(\mathrm{i}\alpha_1)^{-1}U_{TS}^{(1)} \quad \text{with} \quad U_{TS}^{(1)} = \int_{\eta_0}^{\eta} \mathrm{Ai}(\eta)\mathrm{d}\eta - \frac{\beta^2}{\gamma_1^2}\mathrm{Ai}'(\eta_0)Ł(\eta). \tag{3.78}$$

Consider now the terms $\tilde{U}_2$, $\tilde{V}_2$ and $\tilde{W}_2$ in the expansion (3.62)–(3.65). They are governed by

$$\mathrm{i}\alpha_1\tilde{U}_2 + \tilde{V}_{2,Y} + \mathrm{i}\beta\tilde{W}_2 = -\mathrm{i}\alpha_2 A\tilde{U}_1, \tag{3.79}$$

$$\mathrm{i}(\alpha_1\lambda_0 Y - \omega_1)\tilde{U}_2 + \lambda_0\tilde{V}_2 = -\mathrm{i}\alpha_1\tilde{P}_2 + \tilde{U}_{2,YY} - \mathrm{i}(\alpha_2\lambda_0 Y - \omega_2)A\tilde{U}_1 \tag{3.80}$$

$$\mathrm{i}(\alpha_1\lambda_0 Y - \omega_1)\tilde{W}_2 = -\mathrm{i}\beta\tilde{P}_2 + \tilde{W}_{2,YY} - \mathrm{i}(\alpha_2\lambda_0 Y - \omega_2)A\tilde{W}_1, \tag{3.81}$$

which can be combined to give

$$\left\{\frac{\partial^2}{\partial Y^2} - \mathrm{i}(\alpha_1\lambda_0 Y - \omega_1)\right\}\tilde{V}_{2,YY} = \mathrm{i}(\alpha_2\lambda_0 Y - \omega_2)A\tilde{V}_{1,YY}. \tag{3.82}$$

Equations (3.79) and (3.80) can be used to show that the boundary conditions on the wall, $\tilde{U}_2 = \tilde{V}_2 = \tilde{W}_2 = 0$ at $Y = 0$, are equivalent to

$$\tilde{V}_{2,Y} = 0, \quad \tilde{V}_{2,YYY} = (\alpha_1^2+\beta^2)\tilde{P}_2 + 2\alpha_1\alpha_2 AP_1 \quad \text{at } Y = 0. \tag{3.83}$$

The solution satisfying the first of the above conditions is found to be

$$\tilde{V}_{2,Y} = \left(\frac{\omega_2}{\omega_1} - \frac{\alpha_2}{\alpha_1}\right)\eta_0\left(\mathrm{Ai}(\eta) - \mathrm{Ai}(\eta_0)\right)A + \frac{1}{3}\frac{\alpha_2}{\alpha_1}(\eta\mathrm{Ai}(\eta) - \eta_0\mathrm{Ai}(\eta_0))A + q_2\int_{\eta_0}^{\eta}\mathrm{Ai}(\eta)\,\mathrm{d}\eta, \tag{3.84}$$

where q_2 is a function of x_1, the determination of which is the key task in developing the second-order asymptotic theory of receptivity (see below). Application of the second condition in (3.83) gives

$$(\mathrm{i}\alpha_1\lambda_0)^{2/3}\left\{\left(\frac{\omega_2}{\omega_1} - \frac{2}{3}\frac{\alpha_2}{\alpha_1}\right)\eta_0^2\mathrm{Ai}(\eta_0) + \frac{2}{3}\frac{\alpha_2}{\alpha_1}\mathrm{Ai}'(\eta_0)\right\}A + (\mathrm{i}\alpha_1\lambda_0)^{2/3}q_2\mathrm{Ai}'(\eta_0)$$
$$= (\alpha_1^2+\beta^2)\tilde{P}_2 + 2\alpha_1\alpha_2 AP_1. \tag{3.85}$$

Matching $\tilde{V}_{2,Y}$ with its counterpart in the main deck yields

$$-A\left(\frac{\omega_2}{\omega_1} - \frac{2}{3}\frac{\alpha_2}{\alpha_1}\right)\eta_0\mathrm{Ai}(\eta_0) + q_2\int_{\eta_0}^{\infty}\mathrm{Ai}(\eta)\,\mathrm{d}\eta = -\mathrm{i}\alpha_1\lambda_0 B_2 + \mathrm{i}\gamma_1^2\alpha_1^{-1}\lambda_0 AP_1 J_0. \tag{3.86}$$

After eliminating B_2, P_2 and $\bar{P}_2$ from (3.54)–(3.56) and (3.85)–(3.86) and using (3.75), we arrive at the relation (cf. Smith 1979*a*)

$$\Delta_1(\lambda_0) \equiv a\frac{\alpha_2}{\alpha_1} + \eta_0\mathrm{Ai}(\eta_0)\left(\frac{\lambda_0\omega_1}{\alpha_1\gamma_1} - 1\right)\frac{\omega_2}{\omega_1}$$
$$+\mathrm{i}\lambda_0\alpha_1^{-2}(\mathrm{i}\alpha_1\lambda_0)^{2/3}\left\{\alpha_1(J_\infty - J_0 - I_2) + \frac{2\omega_1}{\gamma_1}\right\}\mathrm{Ai}'(\eta_0) = 0, \tag{3.87}$$

that determines α_2 and ω_2, where

$$a(\lambda_0) = \tfrac{2}{3}\eta_0 \mathrm{Ai}(\eta_0) + \frac{2\alpha_1^2+\beta^2}{\gamma_1^2}\int_{\eta_0}^{\infty}\mathrm{Ai}(\eta)\mathrm{d}\eta + \frac{2}{3}\frac{(\mathrm{i}\alpha_1\lambda_0)^{5/3}}{\alpha_1^2\gamma_1}\left\{\mathrm{Ai}'(\eta_0) - \eta_0^2\mathrm{Ai}(\eta_0)\right\}. \quad (3.88)$$

In terms of η, the spanwise momentum equation (3.81) can be written as

$$[\tilde{W}_{2,\eta\eta} - \eta\tilde{W}_2] = \mathrm{i}\beta(\mathrm{i}\alpha_1\lambda_0)^{-2/3}\tilde{P}_2 + A\left\{\frac{\alpha_2}{\alpha_1}\eta + \eta_0\left(\frac{\omega_2}{\omega_1} - \frac{\alpha_2}{\alpha_1}\right)\right\}\mathrm{i}\beta\gamma_1^{-2}\mathrm{Ai}'(\eta_0)L(\eta). \quad (3.89)$$

The solution may be expressed in the form

$$\tilde{W}_2 = Q_0\mathrm{Ai}(\eta) + Q_1Ł(\eta) + Q_2Ł'(\eta) + Q_3\eta Ł'(\eta). \quad (3.90)$$

Substitution of (3.90) into (3.89) shows that the constants Q_1, Q_2 and Q_3 take the following values respectively:

$$Q_1 = (\mathrm{i}\alpha_1\lambda_0)^{-2/3}\mathrm{i}\beta\tilde{P}_2 - \frac{2}{3}\frac{\alpha_2}{\alpha_1}\frac{\mathrm{i}\beta\mathrm{Ai}'(\eta_0)}{\alpha_1^2+\beta^2}A,$$

$$Q_2 = \left(\frac{\omega_2}{\omega_1} - \frac{\alpha_2}{\alpha_1}\right)\eta_0\frac{\mathrm{i}\beta\mathrm{Ai}'(\eta_0)}{\alpha_1^2+\beta^2}A, \quad Q_3 = \frac{1}{3}\frac{\alpha_2}{\alpha_1}\frac{\mathrm{i}\beta\mathrm{Ai}'(\eta_0)}{\alpha_1^2+\beta^2}A.$$

The boundary condition $\tilde{W}_2 = 0$ at $Y = 0$ fixes Q_0:

$$Q_0 = \frac{1}{\mathrm{Ai}^2}\int_{\eta_0}^{\infty}\mathrm{Ai}(\eta)\,\mathrm{d}\eta\left(\frac{\omega_2}{\omega_1} - \frac{2}{3}\frac{\alpha_2}{\alpha_1}\right)\frac{\mathrm{i}\beta\eta_0\mathrm{Ai}'(\eta_0)}{\alpha_1^2+\beta^2}A.$$

The streamwise velocity $\tilde{U}_2$, which will be needed to define the coupling coefficient, can be calculated by using the continuity equation

$$\tilde{U}_2 = -(\mathrm{i}\alpha_1)^{-1}\left\{\tilde{V}_{2,Y} + \mathrm{i}\beta\tilde{W}_2 + \mathrm{i}\alpha_2\tilde{U}_1\right\}. \quad (3.91)$$

The terms $\tilde{U}_4$, $\tilde{V}_4$ etc, in (3.62)–(3.65) arise as the direct response to the forcing from the upper and edge layers. They are governed by the equations

$$\mathrm{i}\alpha_1\tilde{U}_4 + \tilde{V}_{4,Y} + \mathrm{i}\beta\tilde{W}_4 = -A'(x_1)\tilde{U}_1, \quad (3.92)$$

$$\mathrm{i}(\alpha_1\lambda_0 Y - \omega_1)\tilde{U}_4 + \lambda_0\tilde{V}_4 = -\mathrm{i}\alpha_1 P_4 + \tilde{U}_{4,YY} - \Lambda(x_1)Y\tilde{U}_1 - \lambda_1 x_1\tilde{V}_1 - A'(x_1)\hat{p}_1, \quad (3.93)$$

$$\mathrm{i}(\alpha_1\lambda_0 Y - \omega_1)\tilde{W}_4 = -\mathrm{i}\beta P_4 + \tilde{W}_{4,YY} - \Lambda(x_1)Y\tilde{W}_1, \quad (3.94)$$

where Λ is defined by

$$\Lambda(x_1) = \lambda_0 A'(x_1) + \mathrm{i}\alpha_1\lambda_1 x_1 A. \quad (3.95)$$

The solution is subject to the no-slip condition on the wall and the matching requirement with the main-deck solution, namely

$$\tilde{U}_4 = \tilde{V}_4 = \tilde{W}_4 = 0 \quad \text{at } Y = 0; \quad \tilde{U}_4 \to \lambda_0 B_4 + \lambda_1 x_1 A B_1, \quad \tilde{W}_4 \to 0 \quad \text{as } Y \to \infty.$$

Here the matching condition is derived by expanding the small-y asymptote of the main-deck solution (3.37) about x_0. The above boundary conditions imply that

$$\tilde{V}_{4,Y} \to -\mathrm{i}\alpha_1\lambda_0 B_4 - \Lambda(x_1)B_1 \quad \text{as } Y \to \infty, \quad (3.96)$$

$$\tilde{V}_{4,YYY} = (\alpha_1^2 + \beta^2)P_4 - 2i\alpha_1 A' P_1 \quad \text{at } Y = 0. \tag{3.97}$$

Now eliminating the pressure from (3.92)–(3.94), we can show that $\tilde{V}_{4,YY}$ satisfies

$$\left\{ \frac{\partial^2}{\partial Y^2} - i(\alpha_1 \lambda_0 Y - \omega_1) \right\} \tilde{V}_{4,YY} = \Lambda(x_1) Y \tilde{V}_{1,YY} = \Lambda(x_1)(\eta - \eta_0)\mathrm{Ai}(\eta). \tag{3.98}$$

In order for equation (3.98) to have a solution which also satisfies the boundary conditions (3.96) and (3.97), a solvability condition must be satisfied. This condition follows from applying the boundary and matching conditions to the general solution of (3.98). The latter is found to be

$$\tilde{V}_{4,Y} = \tfrac{1}{3}(i\alpha_1\lambda_0)^{-1}\Lambda(x_1)\{(\eta - 3\eta_0)\mathrm{Ai}(\eta) + 2\eta_0 \mathrm{Ai}(\eta_0)\} + q_4 \int_{\eta_0}^{\eta} \mathrm{Ai}(\eta)\, d\eta, \tag{3.99}$$

where q_4 is an unknown function of x_1. The boundary conditions (3.96)–(3.97) lead to

$$\tfrac{2}{3}(i\alpha_1\lambda_0)^{-1}\Lambda\eta_0 \mathrm{Ai}(\eta_0) + q_4 \int_{\eta_0}^{\infty} \mathrm{Ai}(\eta)\, d\eta = -i\alpha_1\lambda_0 B_4 - \Lambda B_1, \tag{3.100}$$

$$\tfrac{2}{3}(i\alpha_1\lambda_0)^{-1/3}\Lambda\left\{\mathrm{Ai}'(\eta_0) - \eta_0^2 \mathrm{Ai}(\eta_0)\right\} + (i\alpha_1\lambda_0)^{2/3} q_4 \mathrm{Ai}'(\eta_0) = (\alpha_1^2 + \beta^2)P_4 - 2i\alpha_1 A' P_1. \tag{3.101}$$

Eliminating B_4 and P_4 from (3.57), (3.100)–(3.101), and using (3.74)–(3.75), we obtain

$$A'(x_1) = \sigma x_1 A + N\, e^{i\alpha_d x_1} \tag{3.102}$$

where

$$\sigma = -i\alpha_1\lambda_1 b/(a\lambda_0), \quad N = \lambda_0 F_v / a, \tag{3.103}$$

with a and F_v being given by (3.88) and (3.59), and

$$b = \tfrac{2}{3}\eta_0 \mathrm{Ai}(\eta_0) - \int_{\eta_0}^{\infty} \mathrm{Ai}(\eta) d\eta + \frac{2}{3}\frac{(i\alpha_1\lambda_0)^{5/3}}{\alpha_1^2\gamma_1}\{\mathrm{Ai}'(\eta_0) - \eta_0^2 \mathrm{Ai}(\eta_0)\}.$$

As has been indicated earlier, there are two factors that make a contribution of $O(R^{-1/8})$ to the receptivity: the $O(R^{-1/8})$ forcing term and the $O(R^{-1/8})$ correction to the T-S wave solution. The key task in including these higher-order effects is to determine the unknown function $q_2(x_1)$; see (3.84). To this end, we must consider the terms with the subscript '5' in the expansion. One can readily write down the governing equations for $\tilde{U}_5$, $\tilde{V}_5$ and $\tilde{W}_5$, from which it follows that $\tilde{V}_5$ satisfies

$$\left\{ \frac{\partial^2}{\partial Y^2} - i(\alpha_1\lambda_0 Y - \omega_1) \right\} \tilde{V}_{5,YY} = Y\left(\lambda_0 \frac{\partial}{\partial x_1} + i\alpha_1\lambda_1 x_1\right) \tilde{V}_{2,YY} + i\alpha_2\lambda_1 x_1 A Y \tilde{V}_{1,YY} + i(\alpha_2\lambda_0 Y - \omega_2)\tilde{V}_{4,YY}. \tag{3.104}$$

Inserting (3.84) and (3.99) into (3.104) and solving the resulting equation, we find

$$\tilde{V}_{5,Y} = \tilde{G}_V(\eta) + q_5 \int_{\eta_0}^{\eta} \mathrm{Ai}(\eta) d\eta, \tag{3.105}$$

where q_5 is an unknown function of x_1, and

$$\begin{aligned}\tilde{G}_V = (\mathrm{i}\alpha_1\lambda_0)^{-1}\Lambda\Bigg\{&\frac{1}{9}\frac{\alpha_2}{\alpha_1}\int_{\eta_0}^{\eta}[\eta^3\mathrm{Ai}(\eta)-2\mathrm{Ai}(\eta)]\,\mathrm{d}\eta\\&+\frac{1}{3}\left(\frac{\omega_2}{\omega_1}-\frac{2\alpha_2}{\alpha_1}\right)\eta_0\int_{\eta_0}^{\eta}[\eta^2\mathrm{Ai}(\eta)-\mathrm{Ai}'(\eta)]\,\mathrm{d}\eta-\left(\frac{\omega_2}{\omega_1}-\frac{\alpha_2}{\alpha_1}\right)\eta_0^2\left(\mathrm{Ai}'(\eta)-\mathrm{Ai}'(\eta_0)\right)\Bigg\}\\&+q_4\left\{\frac{1}{3}\frac{\alpha_2}{\alpha_1}(\eta\mathrm{Ai}(\eta)-\eta_0\mathrm{Ai}(\eta_0))+\left(\frac{\omega_2}{\omega_1}-\frac{\alpha_2}{\alpha_1}\right)\eta_0(\mathrm{Ai}(\eta)-\mathrm{Ai}(\eta_0))\right\}\\&+\tfrac{1}{3}(\mathrm{i}\alpha_1\lambda_0)^{-1}\Lambda_1\left\{(\eta-3\eta_0)\mathrm{Ai}(\eta)+2\eta_0\mathrm{Ai}(\eta_0)\right\},\end{aligned}\tag{3.106}$$

with

$$\Lambda_1 = \lambda_0 q_2' + \mathrm{i}\alpha_1\lambda_1 x_1 q_2 + \mathrm{i}\alpha_2\lambda_1 x_1 A.$$

The boundary condition at $Y = 0$ leads to

$$\begin{aligned}&-(\mathrm{i}\alpha_1\lambda_0)^{-1/3}\Lambda\left\{\frac{2}{9}\frac{\alpha_2}{\alpha_1}(\eta_0^3\mathrm{Ai}'(\eta_0)+\mathrm{Ai}'(\eta_0))+\frac{2}{3}\left(\frac{\omega_2}{\omega_1}-\frac{\alpha_2}{\alpha_1}\right)\eta_0^2(\eta_0\mathrm{Ai}'(\eta_0)+\mathrm{Ai}(\eta_0))\right\}\\&+q_4\left\{\left(\frac{\omega_2}{\omega_1}-\frac{2}{3}\frac{\alpha_2}{\alpha_1}\right)\eta_0^2\mathrm{Ai}(\eta_0)+\frac{2}{3}\frac{\alpha_2}{\alpha_1}\mathrm{Ai}'(\eta_0)\right\}(\mathrm{i}\alpha_1\lambda_0)^{2/3}\\&+\tfrac{2}{3}(\mathrm{i}\alpha_1\lambda_0)^{-1/3}\Lambda_1\left(\mathrm{Ai}'(\eta_0)-\eta_0^2\mathrm{Ai}(\eta_0)\right)+(\mathrm{i}\alpha_1\lambda_0)^{2/3}q_5\mathrm{Ai}'(\eta_0)\\&=(\alpha_1^2+\beta^2)\tilde{P}_5+2\alpha_1\alpha_2 P_4-2\mathrm{i}\alpha_1\tilde{P}_{2,x_1}-2\mathrm{i}\alpha_2 A'(x_1)P_1.\end{aligned}\tag{3.107}$$

On the other hand, matching $\tilde{V}_{5,Y}$ with its counterpart in the main deck, we find

$$\begin{aligned}&-\mathrm{i}\alpha_1\lambda_1 x_1 B_2-\mathrm{i}\alpha_1\lambda_0 B_5+\left[\mathrm{i}\gamma_1^2\alpha_1^{-1}P_4+\left(1-\frac{\beta^2}{\alpha_1^2}\right)A'P_1\right]\lambda_0 J_0\\&=(\mathrm{i}\alpha_1\lambda_0)^{-1}\Lambda\left\{\frac{1}{9}\frac{\alpha_2}{\alpha_1}(-\eta_0^2\mathrm{Ai}'(\eta_0)+2\eta_0\mathrm{Ai}(\eta_0))+\frac{2}{3}\left(\frac{\omega_2}{\omega_1}-\frac{2\alpha_2}{\alpha_1}\right)\eta_0\mathrm{Ai}(\eta_0)\right.\\&\left.+\frac{1}{3}\left(\frac{2\omega_2}{\omega_1}-\frac{\alpha_2}{\alpha_1}\right)\eta_0^2\mathrm{Ai}'(\eta_0)\right\}\\&-q_4\left(\frac{\omega_2}{\omega_1}-\frac{2}{3}\frac{\alpha_2}{\alpha_1}\right)\eta_0\mathrm{Ai}(\eta_0)+\tfrac{2}{3}(\mathrm{i}\alpha_1\lambda)^{-1}\Lambda_1\eta_0\mathrm{Ai}(\eta_0)+q_5\int_{\eta_0}^{\infty}\mathrm{Ai}(\eta)\,\mathrm{d}\eta.\end{aligned}\tag{3.108}$$

After eliminating $\bar{P}_5$, $\tilde{P}_5$ and B_5 among (3.55), (3.58), and (3.107)–(3.108), and making use of (3.75) and (3.100)–(3.101), we arrive at the key equation that determines $q_2(x_1)$, namely

$$aq_2' + b(\mathrm{i}\alpha_1\lambda_1/\lambda_0)x_1 q_2 = r_0\Lambda + r_1\lambda_0 A' + r_2(\mathrm{i}\alpha_1\lambda_1 x_1)A + \lambda_0 F_c,\tag{3.109}$$

where F_c is given by (3.60), and the constants r_0, r_1 and r_2 are given by (B 1)–(B 3) in Appendix B. After substituting in (3.102), equation (3.109) can be written as

$$q_2' = \sigma x_1 q_2 + \sigma_1 x_1 A + \tau N\,\mathrm{e}^{\mathrm{i}\alpha_d x_1}\tag{3.110}$$

with

$$\sigma_1 = [(\mathrm{i}\alpha_1\lambda_1)(r_0+r_2)+\lambda_0(r_0+r_1)\sigma]/a, \quad \tau = \lambda_0(r_0+r_1)/a + F_c/F_v.\tag{3.111}$$

The amplitude equations (3.102) and (3.110) form the basis for the calculation of the initial amplitude of the T-S wave and the coupling coefficient.

3.5. *Downstream development and the coupling coefficient*

We now show how the amplitude equations (3.102) and (3.110) can be used to obtain the initial amplitude of the T-S wave and the coupling coefficient. The appropriate solution to (3.102) is (cf. Wu 1999)

$$A(x_1) = N \exp\left(\tfrac{1}{2}\sigma x_1^2\right) \int_{-\infty}^{x_1} \exp\left(-\tfrac{1}{2}\sigma\xi^2 + \mathrm{i}\alpha_d\xi\right) \mathrm{d}\xi, \tag{3.112}$$

and has the property that as $x_1 \to -\infty$,

$$A(x_1) \to (N\,\mathrm{e}^{\mathrm{i}\alpha_d x_1}/\sigma)(-x_1)^{-1} + O(x_1)^{-2}.$$

As was shown in Wu (1999), the above behaviour of $A(x_1)$ in fact matches with the leading-order forced response upstream; see also Appendix C. On the other hand, as $x_1 \to \infty$

$$A(x_1) \to A_\infty \exp\left(\tfrac{1}{2}\sigma x_1^2\right), \quad \text{with} \quad A_\infty = N \int_{-\infty}^{\infty} \exp\left(-\tfrac{1}{2}\sigma\xi^2 + \mathrm{i}\alpha_d\xi\right) \mathrm{d}\xi. \tag{3.113}$$

On inserting (3.112) into (3.110), it can be shown that

$$q_2 = N\left\{\sigma_1 \int_{-\infty}^{x_1} \eta \int_{-\infty}^{\eta} \exp\left(-\tfrac{1}{2}\sigma\xi^2 + \mathrm{i}\alpha_d\xi\right) \mathrm{d}\xi\mathrm{d}\eta + \tau \int_{-\infty}^{x_1} \exp\left(-\tfrac{1}{2}\sigma\xi^2 + \mathrm{i}\alpha_d\xi\right) \mathrm{d}\xi\right\} \exp\left(\tfrac{1}{2}\sigma x_1^2\right), \tag{3.114}$$

from which it follows that as $x_1 \to -\infty$,

$$q_2 \to \left\{\frac{\lambda_0(r_0 + r_2)}{b}(N/\sigma) - \frac{\lambda_0^2 F_c}{\mathrm{i}\alpha_1\lambda_1 b}\right\}(-x_1)^{-1}\,\mathrm{e}^{\mathrm{i}\alpha_d x_1}, \tag{3.115}$$

where use has been made of (3.111) and (3.103). It is shown in Appendix C that q_2 matches to the upstream forced response at the second order.

In the downstream limit, $x_1 \to \infty$,

$$q_2 \to (\tfrac{1}{2}\sigma_1 x_1^2 + q_\infty) A_\infty \exp(\tfrac{1}{2}\sigma x_1^2) \tag{3.116}$$

where

$$q_\infty = -\frac{\sigma_1}{2\sigma}\left(1 - \frac{\alpha_d^2}{\sigma}\right) + \tau. \tag{3.117}$$

As is indicated by (3.62), the streamwise velocity of the TS wave, up to $O(R^{-1/8})$ accuracy, is given by

$$u_{TS} = \epsilon_c h R^{1/16}(A(x_1)\tilde{U}_1 + \epsilon\tilde{U}_2)E, \tag{3.118}$$

and after substituting in (3.78), (3.84)–(3.85), (3.90)–(3.91), and making use of (3.113) and (3.116), we obtain that as $x_1 \to \infty$,

$$u_{TS} \to \epsilon_c h R^{1/16}(-\mathrm{i}\alpha_1)^{-1} A_\infty \left\{U_{TS}^{(2)} + \tfrac{1}{2}\epsilon\sigma_1 x_1^2 U_{TS}^{(1)}\right\} \exp(\tfrac{1}{2}\sigma x_1^2)E \tag{3.119}$$

where $U_{TS}^{(1)}$ and $U_{TS}^{(2)}$ are given by (3.78) and (B 4) respectively.

As $x_1 = O(R^{3/16})$, the T-S wave eventually acquires an $O(1)$ growth rate, and evolves over the fast streamwise scale $\bar{x}$. The direct external forcing becomes unimportant, with the result that the T-S wave is described by the free-evolution theory, i.e. the local parallel stability theory. The T-S wave solution, its streamwise velocity in the

lower deck say, takes the usual WKBJ form

$$u_{TS} = A_I U_{TS}(Y, x; \epsilon) \exp\left\{ \mathrm{i}R^{3/8} \int_{x_0}^{x} \alpha_{TS}(x)\, \mathrm{d}x - \mathrm{i}\omega \bar{t} \right\} \tag{3.120}$$

where the constant A_I represents the (unknown) amplitude of the T-S wave. The complex wavenumber $\alpha_{TS}(x)$ has the expansion

$$\alpha_{TS} = \alpha_1(x) + \epsilon\alpha_2(x) + \cdots$$

with α_1, α_2 etc. being determined by an eigenvalue problem, in which the dependence on the slow variable x is parametric. As $x - x_0 = O(R^{-3/16})$, α_1 and α_2 can be approximated by their Taylor series; using this in (3.120) we find that

$$\begin{aligned} u_{TS} &\approx A_I U_{TS}(Y, x_0; \epsilon) \exp\{\tfrac{1}{2}\alpha_1'(x_0)x_1^2 + \tfrac{1}{2}\epsilon\alpha_2'(x_0)x_1^2\} E \\ &\approx A_I U_{TS}(Y, x_0; \epsilon) \left(1 + \tfrac{1}{2}\epsilon\alpha_2'(x_0)x_1^2\right) \mathrm{e}^{\frac{1}{2}\alpha_1'(x_0)x_1^2} E. \end{aligned} \tag{3.121}$$

Matching the leading terms in (3.119) and (3.121) gives

$$u_I \equiv A_I U_{TS}(Y, x_0; \epsilon) = \epsilon_c h R^{1/16} (-\mathrm{i}\alpha_1)^{-1} A_\infty U_{TS}. \tag{3.122}$$

The terms proportional to x_1^2 match automatically since $\sigma = \alpha_1'(x_0)$ and $\sigma_1 = \alpha_2'(x_0)$.

In receptivity experiments, one usually has to measure the streamwise velocity of the T-S wave at some distance downstream of the neutral curve. That velocity is then extrapolated back to give the velocity at the lower-branch neutral point, which is then used to define the receptivity coefficient. In our theory, the u_I given by (3.122) represents exactly this extrapolated velocity. It is worth noting that although u_I is often referred to as the streamwise velocity of the T-S wave at the neutral point on the lower branch, it is *not* the physical velocity measured directly at that point; the latter corresponds to u_{TS} (as defined by (3.118)) evaluated at $x_1 = 0$, and in fact is, to leading order, just half u_I. Interestingly, it is u_I that is needed for the calculation of the continued development of the T-S wave, as (3.120) shows. The physical velocity at the neutral point, on the other hand, cannot be 'fed' as the initial amplitude even if it were available. The reason for this is that near the neutral point, the local stability theory, which unlike (3.102) does not take account of the forcing, is invalid.

To be consistent with the practice in experimental studies, we use the maximum value of u_I as a measure of the T-S wave magnitude. For the vortical disturbance, the amplitude of the generated T-S wave, in general, is dependent on the vertical structure of the gust in the free stream. However, a close examination of the forcing terms, given by (3.59)–(3.60), indicates that such a dependence should be weak. First, if the vertical variation of a gust occurs on the slow variable $\tilde{y} \equiv \epsilon\bar{y}$, then $\bar{u}_c'(\bar{y}) = O(\epsilon)$ and $\bar{R}_p = O(\epsilon)$, implying that the receptivity to leading order depends only on the slip velocity of the gust $\bar{u}_c(0)$, unaffected by the detailed distribution of the gust. A typical case is the one that corresponds to the two-dimensional limit of (3.7) with $\beta_v = O(\epsilon)$, as was considered by Duck *et al.* (1996). If the gust is further assumed to be 'compact' in the vertical direction and centred at a large distance from the wall, at $\bar{y}_c \gg 1$ say, such that $\bar{u}_c$ and $\bar{w}_c$ are nearly uniform away from $\bar{y}_c$, then we may neglect $\bar{u}_c'(0)$ and $\bar{w}_c'(0)$ as well as their higher-order derivatives. The convecting wake in Dietz's (1999) experiments apparently falls into this category. Then by performing repeated integration by parts on the integral on the right-hand side of (3.61), it can be shown that the integral is smaller than ϵ to *any* power. Thus we have

$$\int_0^\infty \bar{R}_p(\bar{y})\, \mathrm{e}^{-\gamma_1 \bar{y}}\, \mathrm{d}\bar{y} \approx \frac{2\epsilon \mathrm{i}\alpha_w}{\alpha_w + \gamma_1} [2\alpha_c \bar{u}_c(0) + \beta \bar{w}_c(0)] \bar{v}_M(0). \tag{3.123}$$

An alternative argument to justify the above approximation goes as follows. Since the integrand in (3.61) involves $\bar{u}_c'$ and $\bar{w}_c'$, the dominant contribution to the integral would come from the region surrounding $\bar{y}_c$. But that contribution should be small because of the factor $\exp(-(\alpha_w+\gamma_1)\bar{y})$ in the integrand. This intuitive consideration may be formalized mathematically by assuming that $\bar{u}_c' = \Phi(\bar{y}-\bar{y}_c)$ with Φ being majorized by $M\exp(-s|\bar{y}-\bar{y}_c|)$ say, that is $|\Phi(\bar{y}-\bar{y}_c)| \leqslant M\exp(-s|\bar{y}-\bar{y}_c|)$, where M and s are positive constants. It follows that

$$\left|\int_0^\infty \bar{u}_c'(\bar{y})\,\mathrm{e}^{-(\alpha_w+\gamma_1)\bar{y}}\,\mathrm{d}\bar{y}\right| \leqslant \frac{2s\,\mathrm{e}^{-(\alpha_1+\gamma_1)\bar{y}_c}-\mathrm{e}^{-s\bar{y}_c}}{s^2-(\alpha_w+\gamma_1)^2}M;$$

the integral is exponentially small if $\bar{y}_c \gg 1$ and hence can be neglected. Similar estimates can be made of the integrals involving $\bar{w}_c'$ and $y\bar{R}_p$.

For a 'compact' two-dimensional vortical disturbance, the forcing term is proportional to $\bar{u}_c(0)$, i.e. $A_\infty = \bar{u}_c(0)A_\infty^{(2)}$. We may define the coupling coefficient C_V as

$$C_V \equiv \max|u_I|/\epsilon_c\bar{u}_c(0) = R^{1/16}hA_\infty^{(2)}\max_\eta|U_{TS}| = R^{-5/16}R_hA_\infty^{(2)}\alpha_1^{-1}\max_\eta|U_{TS}|, \tag{3.124}$$

where $R_h = U_\infty h^*/\nu$ is the roughness Reynolds number based on the dimensional roughness height h^*.

For a 'compact' three-dimensional vortical disturbance, we find that to $O(\epsilon)$ accuracy, $A_\infty = \{\bar{u}_c(0)+\epsilon\beta\bar{w}_c(0)/(\alpha_w+\gamma_1)\}A_\infty^{(3)}$. The coupling coefficient C_V can be defined as

$$C_V^{(3)} \equiv \frac{\max|u_I|}{\epsilon_c[\bar{u}_c(0)+\epsilon\beta\bar{w}_c(0)/(\alpha_w+\gamma_1)]} = R^{-5/16}R_hA_\infty^{(3)}\alpha_1^{-1}\max_\eta|U_{TS}|. \tag{3.125}$$

4. Receptivity to acoustic disturbance

4.1. *The upper deck*

For the acoustic disturbance, the leading-order interaction that leads to the generation of T-S waves takes place in the lower deck. But the sound and the mean-flow distortion also interact in the main and upper decks, making an $O(R^{-1/8})$ contribution to the receptivity. In the upper deck, the expansion for the velocity and pressure takes the form

$$u = 1+\epsilon^2h\bar{u}_M\,\mathrm{e}^{\mathrm{i}\alpha_w\bar{x}}+\epsilon_su_\infty\,\mathrm{e}^{-\mathrm{i}\omega\bar{t}}+\epsilon_shR^{1/16}(\bar{u}_1+\epsilon\bar{u}_2+\epsilon^2\bar{u}_3)E \\ +\epsilon\epsilon_sh(\bar{u}_4+\epsilon\bar{u}_5)E+\text{c.c.}+\cdots,$$

$$v = \epsilon^2h\bar{v}_M\,\mathrm{e}^{\mathrm{i}\alpha_w\bar{x}}+\epsilon_shR^{1/16}(\bar{v}_1+\epsilon\bar{v}_2+\epsilon^2\bar{v}_3)E+\epsilon\epsilon_sh(\bar{v}_4+\epsilon\bar{v}_5)E+\text{c.c.}+\cdots,$$

$$p = \epsilon^2h\bar{p}_M\,\mathrm{e}^{\mathrm{i}\alpha_w\bar{x}}+\epsilon\epsilon_s\mathrm{i}\omega u_\infty\bar{x}\,\mathrm{e}^{-\mathrm{i}\omega\bar{t}}+\epsilon_shR^{1/16}(\bar{p}_1+\epsilon\bar{p}_2+\epsilon^2\bar{p}_3)E \\ +\epsilon\epsilon_sh(\bar{p}_4+\epsilon\bar{p}_5)E+\text{c.c.}+\cdots,$$

where the solution for the mean-flow distortion $(\bar{u}_M,\bar{v}_M,\bar{p}_M)$ is given by (2.20). In the present incompressible (i.e. small Mach number) limit, the sound wave is represented by an $O(\epsilon_s)$ uniform pulsation in the streamwise velocity, driven by a uniform pressure gradient. The forcing term due to the sound–roughness interaction has the wavenumber α_w, and we shall allow α_w to differ from the T-S wavenumber α by

$O(R^{-3/16})$; so the detuning parameter

$$\alpha_d \approx R^{3/16}[\alpha_w - (\alpha_1 + \epsilon\alpha_2 + \epsilon^2\alpha_3)]. \tag{4.1}$$

The quantities with subscripts '1', '2' and '3' in the expansion represent the T-S wave and the higher-order corrections. The solutions for them are the two-dimensional version of those in the previous section, and will not be repeated here. But it is worth noting that the magnitude of the T-S wave generated by the sound–roughness interaction is a factor $R^{1/8}$ larger than that generated by the vorticity–roughness interaction. The solutions for $\bar{p}_4$ and $\bar{v}_4$ are the same as (3.20) and (3.22) provided that β and the forcing terms in these equations are set to zero, that is

$$\bar{p}_4 = \left(P_4 + \mathrm{i}A'P_1\bar{y}\right)\mathrm{e}^{-\alpha_1\bar{y}}, \quad \bar{v}_4 = -\mathrm{i}[P_4 + \mathrm{i}A'P_1\bar{y}]\,\mathrm{e}^{-\alpha_1\bar{y}}. \tag{4.2}$$

The pressure $\bar{p}_5$ satisfies the two-dimensional version of (3.25), i.e.

$$\bar{p}_{5,\bar{y}\bar{y}} - \alpha_1^2\bar{p}_5 = 2\alpha_1\alpha_2\bar{p}_4 - 2\mathrm{i}\alpha_1\bar{p}_{2,x_1} - 2\mathrm{i}\alpha_2\bar{p}_{1,x_1}, \tag{4.3}$$

and has the solution

$$\bar{p}_5 = \{\bar{P}_5 - \mathrm{i}\alpha_2A'P_1\bar{y}^2 + (\mathrm{i}\bar{P}_{2,x_1} - \alpha_2P_4)\bar{y}\}\,\mathrm{e}^{-\gamma_1\bar{y}}. \tag{4.4}$$

The expansion of the vertical momentum equation yields

$$\mathrm{i}\alpha_1\bar{v}_5 + \mathrm{i}(\alpha_2 - \omega_1)\bar{v}_4 + \bar{v}_{2,x_1} = -\bar{p}_{5,\bar{y}} - \mathrm{i}\alpha_w u_\infty \bar{v}_M^{(1)}\,\mathrm{e}^{\mathrm{i}\alpha_d x_1},$$

and we find that

$$\bar{v}_5 \to -\mathrm{i}\bar{P}_5 - \mathrm{i}\frac{\omega_1}{\alpha_1}P_4 + \frac{\omega_1}{\alpha_1^2}A'P_1 - \frac{\alpha_w}{\alpha_1}u_\infty\bar{v}_M^{(1)}(0)\,\mathrm{e}^{\mathrm{i}\alpha_d x_1} \quad \text{as } \bar{y} \to 0. \tag{4.5}$$

4.2. *The main-deck solution*

The solution in the main deck expands as

$$u = U_B + \epsilon hU_M + \epsilon_s u_\infty\,\mathrm{e}^{-\mathrm{i}\omega\bar{t}} + \epsilon_s hR^{3/16}[AU_1 + \epsilon U_2 + \epsilon^2U_3]E + \epsilon_s h(U_4 + \epsilon U_5)E + \text{c.c.} + \cdots, \tag{4.6}$$

$$v = \epsilon^2 hV_M + \epsilon_s hR^{1/16}[AV_1 + \epsilon V_2 + \epsilon^2V_3]E + \epsilon\epsilon_s h(V_4 + \epsilon V_5)E + \text{c.c.} + \cdots, \tag{4.7}$$

$$p = \epsilon^2 hP_M + \epsilon\epsilon_s\mathrm{i}\omega u_\infty\bar{x}\,\mathrm{e}^{-\mathrm{i}\omega\bar{t}} + \epsilon_s hR^{1/16}[AP_1 + \epsilon P_2 + \epsilon^2P_3]E + \epsilon\epsilon_s h(P_4 + \epsilon P_5)E + \text{c.c.} + \cdots. \tag{4.8}$$

The mean-flow distortion (U_M, V_M, P_M) is given by (2.12). The solutions for U_4 and V_4 are the same as given by (3.51), and the matching condition with the upper-deck solution gives

$$-\mathrm{i}\alpha_1B_4 - A'B_1 = -\mathrm{i}P_4. \tag{4.9}$$

The governing equations for V_5 and P_5 are

$$U_BV_{5,y} - U_B'V_5 = A'P_1 + \mathrm{i}\alpha_1P_4 - \mathrm{i}\omega_1U_4 + \mathrm{i}\alpha_w u_\infty U_M^{(1)}\,\mathrm{e}^{\mathrm{i}\alpha_d x_1},$$

$$U_B(\mathrm{i}\alpha_1V_4 + A'V_1) + \mathrm{i}\alpha_w u_\infty V_M^{(1)}\,\mathrm{e}^{\mathrm{i}\alpha_d x_1} = -P_{5,y}.$$

We find that

$$V_5 = -\mathrm{i}\alpha_1B_5U_B + \mathrm{i}\omega_1B_4 + (A'P_1 + \mathrm{i}\alpha_1P_4)U_B\int^y\frac{\mathrm{d}y}{U_B^2} - \mathrm{i}\alpha_w u_\infty A_M^{(1)}\,\mathrm{e}^{\mathrm{i}\alpha_d x_1}, \tag{4.10}$$

$$P_5 = \tilde{P}_5 - (\alpha_1^2 B_4 - 2\mathrm{i}\alpha_1 A' B_1)\int_0^y U_B^2\,\mathrm{d}y - \left\{\alpha_w^2 u_\infty A_M^{(1)}\int_0^y U_B\,\mathrm{d}y\right\}\mathrm{e}^{\mathrm{i}\alpha_d x_1}. \tag{4.11}$$

The matching of the pressure and vertical velocity in the main and upper layers requires

$$\bar{P}_5 = \tilde{P}_5 - (\alpha_1^2 B_4 - 2\mathrm{i}\alpha_1 A' B_1)I_2 - \tfrac{1}{2}\alpha_1^2 A B_1 I_2 x_1 - \alpha_w^2 u_\infty A_M^{(1)} I_1\,\mathrm{e}^{\mathrm{i}\alpha_d x_1}, \tag{4.12}$$

$$\begin{aligned}-\mathrm{i}\alpha_1 B_5 + \mathrm{i}\omega_1 B_4 + (A' P_1 + \mathrm{i}\alpha_1 P_4)J_\infty + \tfrac{1}{2}\mathrm{i}\alpha_1 A P_1 J_\infty x_1 \\ = -\mathrm{i}\bar{P}_5 - \mathrm{i}\frac{\omega_1}{\alpha_1}P_4 + \frac{\omega_1}{\alpha_1^2}A' P_1 + \mathrm{i}\alpha_w\left(1+\frac{\alpha_w}{\alpha_1}\right)u_\infty A_M^{(1)}\,\mathrm{e}^{\mathrm{i}\alpha_d x_1}\end{aligned} \tag{4.13}$$

where I_1 is given by (A 2).

4.3. *The lower-deck solution*

For the acoustic disturbance, the lower deck is the most active region in that the sound-roughness interaction there makes the leading-order contribution to the receptivity. The expansion takes the form

$$\begin{aligned}u = \epsilon(\lambda_0 + R^{-3/16}\lambda_1 x_1)Y + \epsilon h\tilde{U}_M\,\mathrm{e}^{\mathrm{i}\alpha_w\bar{x}} + \epsilon_s\tilde{U}_s\,\mathrm{e}^{-\mathrm{i}\omega\bar{t}} \\ + \epsilon_s h R^{3/16}[A(x_1)\tilde{U}_1 + \epsilon\tilde{U}_2 + \epsilon^2\tilde{U}_3]E + \epsilon_s h(\tilde{U}_4 + \epsilon\tilde{U}_5)E + \cdots,\end{aligned} \tag{4.14}$$

$$v = \epsilon^3 h\tilde{V}_M\,\mathrm{e}^{\mathrm{i}\alpha_w\bar{x}} + \epsilon\epsilon_s h R^{1/16}[A(x_1)\tilde{V}_1 + \epsilon\tilde{V}_2 + \epsilon^2\tilde{V}_3]E + \epsilon^2\epsilon_s h(\tilde{V}_4 + \epsilon\tilde{V}_5)E + \cdots, \tag{4.15}$$

$$\begin{aligned}p = \epsilon^2 h\tilde{P}_M\,\mathrm{e}^{\mathrm{i}\alpha_w\bar{x}} + \epsilon\epsilon_s\omega u_\infty\bar{x}\,\mathrm{e}^{-\mathrm{i}\omega\bar{t}} + \epsilon\epsilon_s h R^{3/16}[A(x_1)P_1 + \epsilon\tilde{P}_2 + \epsilon^2\tilde{P}_3]E \\ + \epsilon\epsilon_s h(P_4 + \epsilon\tilde{P}_5)E + \cdots.\end{aligned} \tag{4.16}$$

Here $(\tilde{U}_M, \tilde{V}_M, \tilde{P}_M)$ stands for the solution for the mean-flow distortion as given by (2.24). The $O(\epsilon_s)$ term is the oscillatory flow driven by the unsteady pressure fluctuation

$$\tilde{U}_s = u_\infty\{1 - \exp(\mathrm{i}^{3/2}\omega^{1/2}Y)\}. \tag{4.17}$$

Consider the flow directly forced by the sound–roughness interaction. It is governed by equations

$$\mathrm{i}\alpha_1\tilde{U}_4 + \tilde{V}_{4,Y} = -A'(x_1)\tilde{U}_1, \tag{4.18}$$

$$\begin{aligned}\mathrm{i}(\alpha_1\lambda_0 Y - \omega_1)\tilde{U}_4 + \lambda_0\tilde{V}_4 = -\mathrm{i}\alpha_1 P_4 + \tilde{U}_{4,YY} - \Lambda(x_1)Y\tilde{U}_1 - \lambda_1 x_1\tilde{V}_1 - A'(x_1)P_1 \\ -(\mathrm{i}\alpha_w\tilde{U}_s\tilde{U}_M + \tilde{V}_M\tilde{U}_{s,Y})\,\mathrm{e}^{\mathrm{i}\alpha_d x_1}.\end{aligned} \tag{4.19}$$

Recall that $\tilde{U}_M$ and $\tilde{V}_M$ consist of the $O(\epsilon)$ correction so that the direct forcing term of $O(\epsilon)$ has already been included; this is more convenient than relegating it to the next order. Now under the assumption that $h \ll O(1)$, the boundary conditions on the wall $Y = hF_w(\mathrm{e}^{\mathrm{i}\alpha_w\bar{x}} + \mathrm{c.c.})$ can be replaced by those at $Y = 0$, namely

$$\tilde{U}_4(0) = \mathrm{i}^{3/2}\omega^{1/2}F_w, \quad \tilde{V}_4(0) = 0. \tag{4.20}$$

As usual, eliminating P_4 between (4.18)–(4.19) leads to

$$\left\{\frac{\partial^2}{\partial Y^2} - \mathrm{i}(\alpha_1\lambda_0 Y - \omega_1)\right\}\tilde{V}_{4,YY} = \Lambda(x_1)Y\tilde{V}_{1,YY} - \mathrm{i}\alpha_1(\mathrm{i}\alpha_w\tilde{U}_s\tilde{U}_{M,Y} + \tilde{V}_M\tilde{U}_{s,YY})\,\mathrm{e}^{\mathrm{i}\alpha_d x_1}, \tag{4.21}$$

with Λ being given by (3.95). It is convenient to write

$$\tilde{V}_{4,Y} = \tfrac{1}{3}(\mathrm{i}\alpha_1\lambda_0)^{-1}\Lambda(x_1)\{(\eta - 3\eta_0)\mathrm{Ai}(\eta) + 2\eta_0\mathrm{Ai}(\eta_0)\} + \hat{V}_{4,Y}. \tag{4.22}$$

Then in terms of η, the governing equation for $\hat{V}_{4,\eta\eta}$ becomes

$$\left(\frac{\partial^2}{\partial\eta^2}-\eta\right)\hat{V}_{4,\eta\eta}=-\lambda_0^{-1}(\mathrm{i}\alpha_1\lambda_0)^{-1/3}(\mathrm{i}\alpha_w\tilde{U}_s\tilde{U}_{M,Y}+\tilde{V}_M\tilde{U}_{s,YY})\,\mathrm{e}^{\mathrm{i}\alpha_d x_1}\equiv G(\eta)\,\mathrm{e}^{\mathrm{i}\alpha_d x_1}. \quad (4.23)$$

The matching condition with the main-deck solution is

$$\hat{V}_{4,Y}+\tfrac{2}{3}(\mathrm{i}\alpha_1\lambda_0)^{-1}\Lambda\eta_0\mathrm{Ai}(\eta_0)\to-\mathrm{i}\alpha_1\lambda_0B_4-\Lambda B_1 \quad \text{as } Y\to\infty. \quad (4.24)$$

The boundary conditions (4.20) together with (4.18)–(4.19) imply that

$$\hat{V}_{4,Y}(0)=\mathrm{i}^{1/2}\omega^{1/2}\alpha_1F_w, \quad (4.25)$$

$$\hat{V}_{4,YYY}(0)+\tfrac{2}{3}(\mathrm{i}\alpha_1\lambda_0)^{-1/3}\Lambda(\mathrm{Ai}'(\eta_0)-\eta_0^2\mathrm{Ai}(\eta_0))=\alpha_1^2P_4-2\mathrm{i}\alpha_1A'P_1-\mathrm{i}^{3/2}\omega^{1/2}\omega_1\alpha_1F_w. \quad (4.26)$$

The amplitude equation for $A(x_1)$ can be derived by considering the solvability condition of (4.23)–(4.26). To this end, we multiply both sides of (4.23) by $(\mathrm{Ai}(\eta)+\kappa L(\eta))$ and integrate by parts (Smith 1979*b*), where

$$\kappa=-\mathrm{Ai}'(\eta_0)/Ł'(\eta_0)=\mathrm{Ai}(\eta_0)\mathrm{Ai}'(\eta_0)/\int_{\eta_0}^{\infty}\mathrm{Ai}(\eta)\,\mathrm{d}\eta.$$

After making use of (4.24)–(4.26), we obtain

$$A'=\sigma x_1A+N\,\mathrm{e}^{\mathrm{i}\alpha_d x_1} \quad (4.27)$$

where σ is given in (3.103), and

$$N=-\frac{\mathrm{i}\lambda_0^2}{a\mathrm{Ai}(\eta_0)}\int_{\eta_0}^{\infty}G(\eta)\{\mathrm{Ai}(\eta)+\kappa Ł(\eta)\}\,\mathrm{d}\eta-\frac{\mathrm{i}^{3/2}\omega^{1/2}}{a}(\alpha_1^2-\lambda_0\omega_1)F_w. \quad (4.28)$$

In terms of the Airy function, the solution for $\hat{V}_{4,\eta\eta}$ can be expressed as

$$\hat{V}_{4,\eta\eta}=\mathrm{Ai}(\eta)\int_{\eta_0}^{\eta}\frac{\mathrm{d}q}{\mathrm{Ai}^2(q)}\int_{\infty}^{q}\mathrm{Ai}(q_1)G(q_1)\,\mathrm{d}q_1, \quad (4.29)$$

which is integrated to give

$$\hat{V}_{4,\eta}(\infty)=\int_{\eta_0}^{\infty}\mathrm{Ai}(\eta)\int_{\eta_0}^{\eta}\frac{\mathrm{d}q}{\mathrm{Ai}^2(q)}\int_{\infty}^{q}\mathrm{Ai}(q_1)G(q_1)\,\mathrm{d}q_1\,\mathrm{d}\eta+(\mathrm{i}\alpha_1\lambda_0)^{-1/3}\mathrm{i}^{1/2}\omega^{1/2}\alpha_1F_w. \quad (4.30)$$

The $O(R^{-1/8})$ correction to the receptivity can be obtained by considering $\tilde{V}_5$. Much of the algebra is similar to that for the vortical disturbance. To take the advantage of this similarity, we write

$$\tilde{V}_{5,Y}=\tilde{G}_V+\hat{V}_{5,Y},$$

with $\tilde{G}_V$ being defined by (3.106). It follows that $\hat{V}_5$ satisfies

$$\left(\frac{\partial^2}{\partial\eta^2}-\eta\right)\hat{V}_{5,\eta\eta}=\left\{H(\eta)+\frac{\alpha_2}{\alpha_1}G(\eta)\right\}\mathrm{e}^{\mathrm{i}\alpha_d x_1}, \quad (4.31)$$

where

$$H(\eta)=\left\{\frac{\alpha_2}{\alpha_1}\eta+\left(\frac{\omega_2}{\omega_1}-\frac{\alpha_2}{\alpha_1}\right)\eta_0\right\}\hat{V}_{4,\eta\eta}. \quad (4.32)$$

It can be shown that the boundary conditions are

$$\hat{V}_{5,Y}(0) = \mathrm{i}^{1/2}\omega^{1/2}\alpha_2 F_w, \tag{4.33}$$

$$\hat{V}_{5,YYY}(0) + \tilde{G}_{V,YY}(0) = \alpha_1^2\tilde{P}_5 + 2\alpha_1\alpha_2 P_4 - 2\mathrm{i}\alpha_1\tilde{P}_{2,x_1} - 2\mathrm{i}\alpha_2 A'(x_1)P_1 - \mathrm{i}^{1/2}(\alpha_1\omega_2 + \alpha_2\omega_1)\omega^{1/2}F_w, \tag{4.34}$$

$$\hat{V}_{5,Y} + \tilde{G}_V \to \alpha_1 B_2\lambda_1 x_1 - \mathrm{i}\alpha_1\lambda_0 B_5 + (\alpha_1 P_4 + A'P_1)\lambda_0 J_0 \quad \text{as } Y \to \infty. \tag{4.35}$$

Multiplying both sides of (4.31) by $(\mathrm{Ai}(\eta) + \kappa Ł(\eta))$, integrating from η_0 to ∞ with respect to η and substituting (4.33)–(4.35), (4.24)–(4.26) into the resulting relation, we obtain

$$q_2' = \sigma x_1 q_2 + \sigma_1 x_1 A + \tau N\,\mathrm{e}^{\mathrm{i}\alpha_d x_1} \tag{4.36}$$

where the constants σ and σ_1 are defined by (3.103) and (3.111) respectively, and

$$\tau = \lambda_0(r_0 + r_1)/a + N_c/N$$

with r_0 and r_1 being given by the two-dimension version of (B 1)–(B 2) and

$$\begin{aligned} N_c = {} & -\frac{\mathrm{i}\lambda_0^2}{a\mathrm{Ai}(\eta_0)}\int_{\eta_0}^{\infty}\left\{H(\eta) + \frac{\alpha_2}{\alpha_1}G(\eta)\right\}(\mathrm{Ai}(\eta) + \kappa Ł(\eta))\,\mathrm{d}\eta \\ & -\frac{\mathrm{i}^{3/2}\omega^{1/2}}{a}[\alpha_1\alpha_2 - \lambda_0\alpha_1^{-1}(\alpha_1\omega_2 + \alpha_2\omega_1)]F_w - \frac{\lambda_0\alpha_1\alpha_w}{a}\left(\alpha_w I_1 + 1 + \frac{\alpha_w}{\alpha_1}\right)A_M^{(1)} \\ & -\frac{\lambda_0}{a}\left\{\frac{2\alpha_2 - \omega_1}{\alpha_1} - \alpha_1(J_\infty - J_0)\right\}\left\{-\frac{\mathrm{i}\lambda_0}{\mathrm{Ai}(\eta_0)}\int_{\eta_0}^{\infty}\mathrm{Ai}(\eta)G(\eta)\mathrm{d}\eta + \mathrm{i}^{3/2}\omega^{1/2}\omega_1 F_w\right\} \\ & -\frac{\mathrm{i}\alpha_1}{a}\left(\alpha_1 I_2 - \frac{\omega_1}{\alpha_1}\right)(\mathrm{i}\alpha_1\lambda_0)^{1/3}\hat{V}_{4,\eta}(\infty). \end{aligned} \tag{4.37}$$

We have derived the required amplitude equations (4.27) and (4.36) for the acoustic receptivity, with all the coefficients being given in closed forms. By a similar argument as in § 3.5, the streamwise velocity of the T-S wave at the lower-branch neutral point is found to be

$$u_I = \epsilon_s h R^{3/16}(-\mathrm{i}\alpha_1)^{-1}A_\infty U_{TS}.$$

Since the forcing term is proportional to u_∞, i.e. $A_\infty = u_\infty A_\infty^{(a)}$, we define the coupling coefficient C_A for the acoustic receptivity as

$$C_A \equiv \max|u_I|/\epsilon_s u_\infty = R^{3/16}hA_\infty^{(a)}\max_\eta|U_{TS}| = R^{-3/16}R_h\alpha_1^{-1}A_\infty^{(a)}\max_\eta|U_{TS}|. \tag{4.38}$$

5. Numerical results and comparison with experiments

We now calculate the initial amplitude of the T-S wave and the coupling coefficient for each of the two receptivity mechanisms. The Blasius profile, and the functions $\mathrm{Ai}(\eta)$ and $Ł(\eta)$ in (3.77) are obtained by a shooting method based on a fourth-order Runge–Kutta method. The various integrals are evaluated using the Trapesiodal rule or Simpson's rule wherever possible.

The higher-order corrections to the neutral frequency and wavenumber are presented in figure 2(*a*, *b*), which shows ω_2 and ω_3, and α_2 and α_3 as functions of the scaled spanwise wavenumber β. It is found that in the large-β limit,

$$\omega_2 \sim 0.618\beta^{-1}, \quad \omega_3 \sim 3.270; \qquad \alpha_2 \sim 0.134\beta^{-2}, \quad \alpha_3 \sim 1.439\beta^{-1}. \tag{5.1}$$

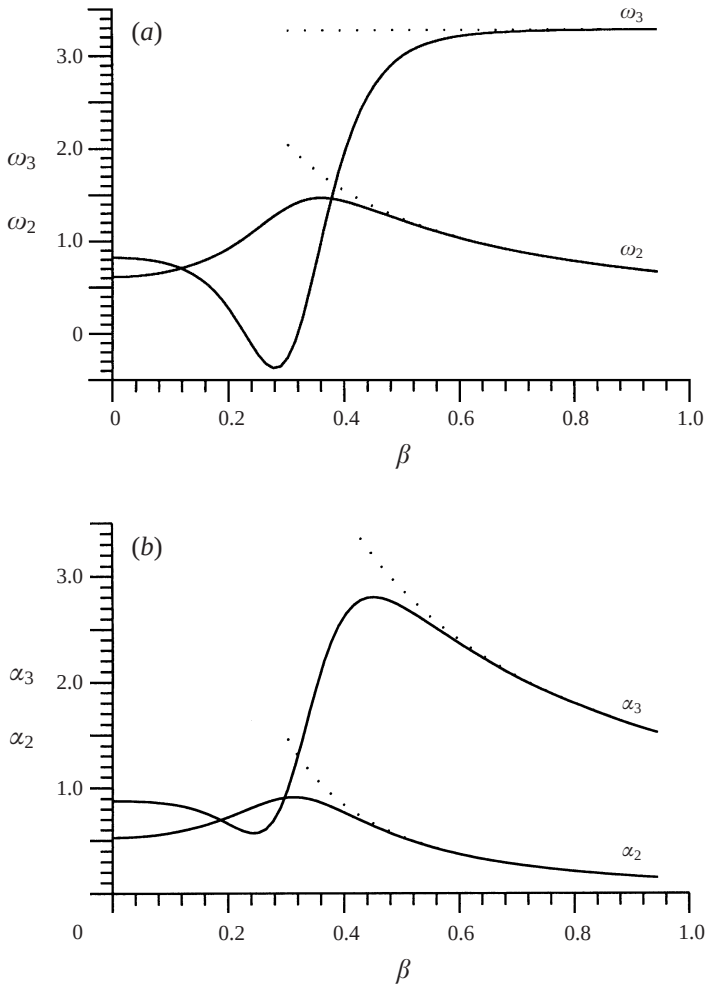

FIGURE 2. Neutral modes of T-S waves: (*a*) variations of ω_2 and ω_3 with β, and (*b*) variations of α_2 and α_3 with β. The dotted lines represent the large-β asymptotes (5.1).

This implies that the expansions (3.3)–(3.4) cease to be valid when $\beta = O(R^{1/8})$, but the pursuit of this limit is beyond the interest of the present paper.

To facilitate the comparison with experiments, we normalized the dimensional frequency of the T-S wave, ω^*, as

$$F = \omega^* \nu / U_\infty^2 \times 10^6.$$

In terms of F, equation (3.4) can be written as

$$F = R^{-3/4}(\omega_1 + \epsilon\omega_2 + \epsilon^2\omega_3 + \cdots) \times 10^6, \tag{5.2}$$

which is the asymptotic approximation to the lower-branch neutral curve. As it stands, this relation is often viewed as approximating the frequency of the neutral T-S wave for a given (but large) Reynolds number. An alternative (and more useful) interpretation is that it determines the neutral Reynolds number (i.e. neutral point x_0) for a given frequency F. The latter viewpoint will be adopted in performing the comparison with experiments. This means that the input data are taken to be the frequency F while R takes the value that satisfies (5.2). It is well known that the R

predicted in this way is rather poor. This inaccuracy will of course have an adverse effect on the prediction of receptivity, but the scaling relations (3.124) and (4.38) suggest that the magnitude of the T-S wave should not be sensitive to the error in R.

Before we present the quantitative results, it is worth noting that (3.124) and (4.38) together with (5.2) show that for roughness of fixed height, the vortical and acoustic coupling coefficients C_V and C_A scale with the frequency F as follows:

$$C_V \sim F^{1/4}, \quad C_A \sim F^{5/12}. \tag{5.3}$$

These imply that for both gust–roughness and sound–roughness interactions, higher frequency components of the free-stream disturbance are more effective in generating T-S waves. This is in contrast to the receptivity mechanism due to the sound–gust interaction where the lower-frequency components are more efficient since the coupling coefficient there is proportional to $F^{-1/2}$ (Wu 1999).

5.1. *Vortical receptivity*

In the experiments on distributed receptivity, the wall roughness is modelled by strips of polyester tape, which are equally spaced near the lower branch of the neutral stability curve. This produces an approximate square-wave, whose first Fourier component is given by $h^* F_w$ with

$$F_w = \frac{2}{\pi} \sin \frac{d^*}{l^*} \pi,$$

where h^* and d^* denote the thickness and width of the tape respectively, and l^* is the separation between the two adjacent strips and is usually taken to be $2d^*$ (i.e. $l^* = 2d^*$) so as to maximize F_w. In Dietz's (1999) experiments, $h^* = 100\,\mu\text{m}$ and $d^* = 25.4\,\text{mm}$. Measurements were carried out for vortical disturbances with frequency F in the range 35 to 70, with the receptivity being found to be the strongest at $F \approx 50$. We calculate the initial T-S wave amplitude for the experimental condition. In figure 3(a), our theoretical results are compared with Dietz's data. We also include the prediction by the 'first-order theory', which is obtained by neglecting the $O(\epsilon)$ term in (B 4). Clearly, the second-order theory outperforms the first-order theory. The overall agreement between the second-order theory and experiments is good. In particular the maximum response is predicted with a remarkable accuracy. However, the optimal frequency given by our theory is $F_c = 47$ as opposed to the experimental value $F_c = 50$. This discrepancy occurs because, for a given F, the neutral Reynolds number and neutral wavenumber predicted by (5.2) and (3.3) are not accurate enough, thereby causing an error in the detuning parameter α_d (see (3.9)). This inaccuracy of the theoretical optimal frequency accounts for the relatively poor pointwise agreement in figure 3(a). Its effect on the receptivity can be removed by plotting the predicted and measured amplitudes of the T-S waves against their respective 'frequency detuning parameter' $\sigma_F = (F - F_c)/F_c$. As is shown in figure 3(b), an excellent pointwise agreement is then obtained. The apparent discrepancy at large σ_F is expected since our perturbation approach is valid only when the frequency is relatively close to the optimal one. Note that the present quantitative comparison with experiments is the first to be made for the distributed receptivity to vortical disturbances. Previously, Dietz (1999) compared his measurements with the finite-Reynolds-number calculations of Choudhari (1996) and the asymptotic result of Kerschen (1991), but only for the localized receptivity; the agreement there was encouraging but somewhat less satisfactory than here.

The above calculations are carried out for a fixed wavelength of the wavy wall, for which the receptivity is most effective (i.e. $\alpha_d = 0$) when the frequency $F \approx 50$.

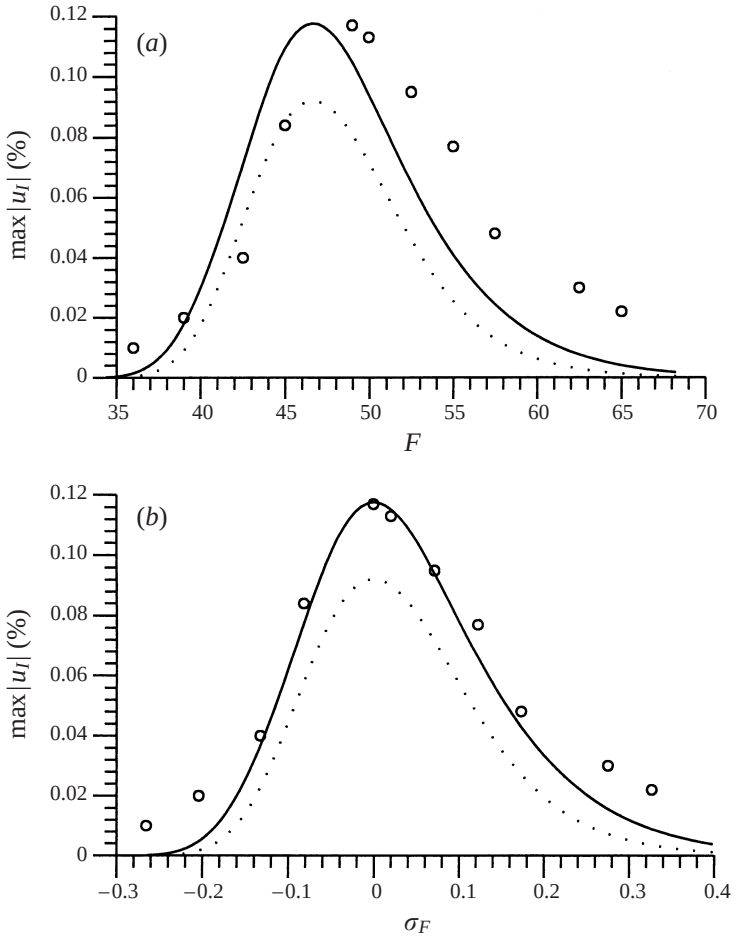

FIGURE 3. (*a*) Variation of the T-S wave amplitude with the forcing frequency F. (*b*) Variation of the T-S wave amplitude with the frequency detuning parameter σ_F. The solid line represents the results given by the second-order theory, and the dotted line by the 'first-order' theory. The symbols correspond to the measurement of Dietz (1999).

In order to have a more complete understanding about the effectiveness of the vortical receptivity, calculations are carried out for different frequencies of the vortical disturbance, for each of which the wavelength of the wall is varied accordingly so as to satisfy $\alpha_d = 0$, thereby achieving the maximum receptivity. The effectiveness can be characterized by the *efficiency function* defined as

$$\Lambda_F = C_V/(F_w R_h),$$

which unlike the coupling coefficient, is independent of the roughness height. The result is displayed in figure 4, which shows that Λ_F increases with the frequency F.

In reality, vortical disturbances are three-dimensional. Unfortunately no controlled experiments have been undertaken yet. But based on the success of Dietz's experiments, it might be possible to generate a vortical disturbance in the form of a three-dimensional convecting wake, for instance by having the vibrating ribbon make a suitable angle to the oncoming flow, or by attaching tapes along the span of the ribbon. With such a possibility in mind, calculations are carried out for this form of disturbance. The variation of efficiency function $\Lambda_F = C_V^{(3)}/(R_h F_w)$ with the spanwise

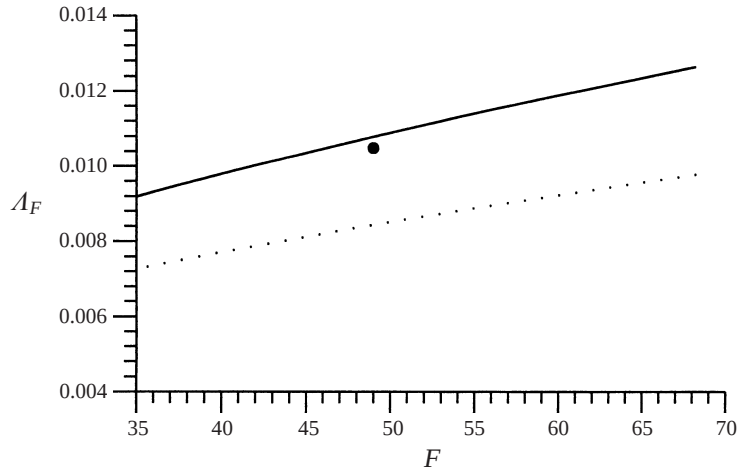

FIGURE 4. The variation of the maximum efficiency function Λ_F (attained when $\alpha_d = 0$) with the forcing frequency F. The solid line represents results from the second-order theory and the dotted line first-order theory. Dietz's (1999) experimental result is marked by ●.

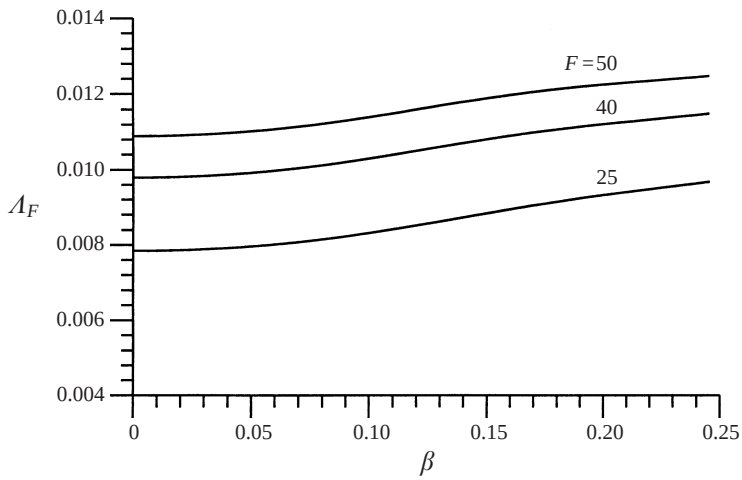

FIGURE 5. Effect of the three-dimensionality receptivity: variation of the maximum efficiency function Λ_F with β.

wavenumber β is shown in figure 5, where $C_V^{(3)}$ is defined by (3.125). As is illustrated, for a fixed F the receptivity becomes more effective as three-dimensionality increases. It must be pointed out, however, that the results presented here are only for β up to a rather moderate value because expansions (3.3)–(3.4) become disordered for larger β. The receptivity to highly oblique disturbances thus requires further investigation. Figure 5 also shows that as with the two-dimensional case, high-frequency disturbances are more efficient in generating T-S waves.

We now consider the receptivity to the vortical disturbance that is the superposition of the form (3.7) with $\pm\beta_v$. This type of vortical disturbance has been much studied (e.g. Crouch 1994; Duck *et al.* 1996). In this case, the approximation (3.123) is invalid, but the bulk contribution represented by the integrals in (3.59)–(3.60) can be evaluated. Because u_∞ cannot be an appropriate characteristic velocity of the fluctuation when β_v is very small, we define the efficiency function as

$$\Lambda_F = \max |u_I| / (\epsilon_c (\overline{\boldsymbol{u}^2}_\infty)^{1/2} R_h F_w),$$

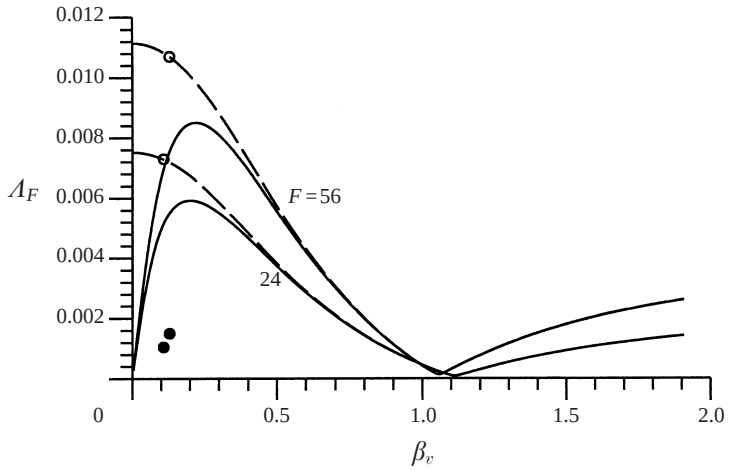

FIGURE 6. Receptivity to the vortical disturbance (3.7): variation of the maximum efficiency function Λ_F with the vertical wavenumber β_v. The solid line: normalized by $(\overline{u^2}_\infty)^{1/2}$, and the dashed line: normalized by u_∞. The results of Crouch (1994) are represented by ●; the open circles show our corresponding results.

where $(\overline{u^2}_\infty)^{1/2}$ is the root-mean-square value of the free-stream fluctuation. In figure 6, we plot the efficiency function against β_v, the vertical wavenumber of the gust, for $F = 56$ and $F = 24$, with the wavelength of the wall roughness being tuned such that $\alpha_d = 0$. The receptivity appears to be selective with respect to β_v, being strongest at $\beta_v \approx 0.3$. At the large β_v-limit, Λ_F approaches a constant value, which is about a third of its peak value. A comparison with figure 4 indicates that this form of gust is just as effective as the convecting wake. For the purpose of comparing with previous calculations of Crouch (1994), we also present the efficiency function based on u_∞, to ensure that the same normalization is used. The open circles correspond to $\beta_v = \epsilon\alpha_c$, the case considered by Crouch (1994). But his result, represented here by the two solid dots, is only 1/7 of ours. A more detailed comparison with Crouch (1994) is shown in figure 7 for the detuned case ($\alpha_d \neq 0$) for $F = 56$ and $F = 24$, taken from his figure 8. Note that due to different ways of normalization, the α_w and A_I in his figure correspond to our $1000R^{-5/8}\alpha_w$ and $1000\Lambda_F$ respectively.

5.2. *Acoustic receptivity*

The efficiency function for the acoustic receptivity can be defined as $\Lambda_F = C_A/(R_h F_w)$. As a check, in figure 8 we compare our results with those of Choudhari (1993). A fair agreement can be observed. Interestingly and somewhat surprisingly, our first-order theory agrees better with his results. As we stated in § 1, Choudhari's calculations were based on the O-S equations. Unlike for the vortical receptivity, the use of the O-S equations for the acoustic receptivity appears better justified. Indeed the result given by this approach may be regarded as a kind of 'composite' approximation, valid up to and including $O(R^{-2/8})$, that is just before the non-parallelism makes an $O(R^{-3/8}\log R^{-1/8})$ correction (Smith 1979*a*). One may argue that his results might be more accurate than ours. Because rather different formulations are adopted in the present and Choudhari's work, it is not possible to make a detailed correspondence so as to identify the source of the discrepancy between his result and our second-order approximation. We note that for the isolated receptivity, Choudhari & Streett (1992) made a detailed comparison between the results given by asymptotic and finite-Reynolds-number methods.

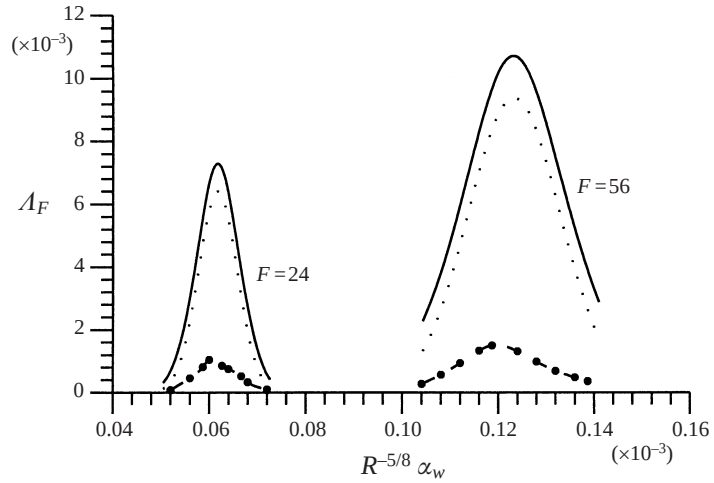

FIGURE 7. Comparison with Crouch's (1994) results (●) with the present results (dotted and solid lines) for (*a*) $F = 56$, and (*b*) $F = 24$.

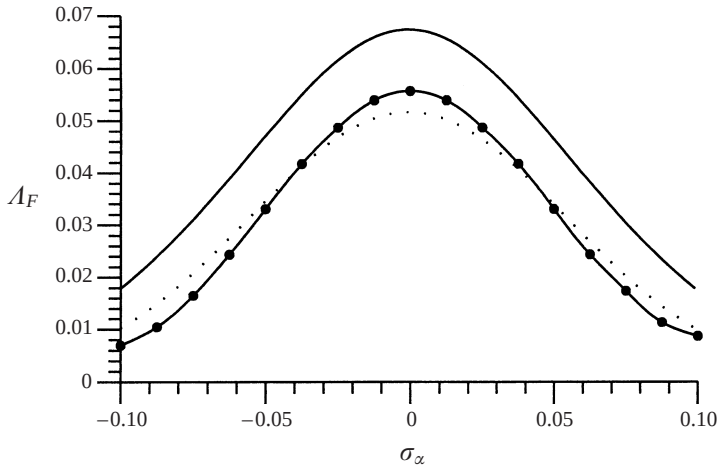

FIGURE 8. Acoustic receptivity: the efficiency function Λ_F vs. the wavenumber detuning parameter $\sigma_\alpha \equiv (\alpha_w - \alpha)/\alpha$, and comparison with Choudhari's results (—●— — —●——) for $F = 55$. First-order theory: the dotted line. The second-order theory: the solid line.

The complete data for the distributed acoustic receptivity came from the experiments of Wiegel & Wlezien (1993), which were conducted using Choudhari's (1993) theoretical results as guidance. Wiegel & Wlezien were the first to simulate the distributed roughness by arrays of tapes, a technique that was later employed by Dietz (1999) to study the vortical receptivity. In their experiments, $h^* = 40\,\mu\text{m}$ and $d^* = 25.4\,\text{mm}$. A loudspeaker produces a sound wave of constant dimensional frequency (80 Hz). The free-stream velocity is adjusted as so to vary the non-dimensional frequency F. Wiegel & Wlezien mentioned that the temperature was maintained at an almost constant level, but did not give its value in their paper. Using the data in their figure 14, we are able to deduce that the kinematic viscosity $\nu = 1.546 \times 10^{-5}\,\text{m}^2\,\text{s}^{-1}$, suggesting that the temperature is about 25 °C. We calculate the coupling coefficient for the above parameters. A comparison with their measurements is made in figure 9. Our first-order approximation shows an excellent agreement with the experiments.

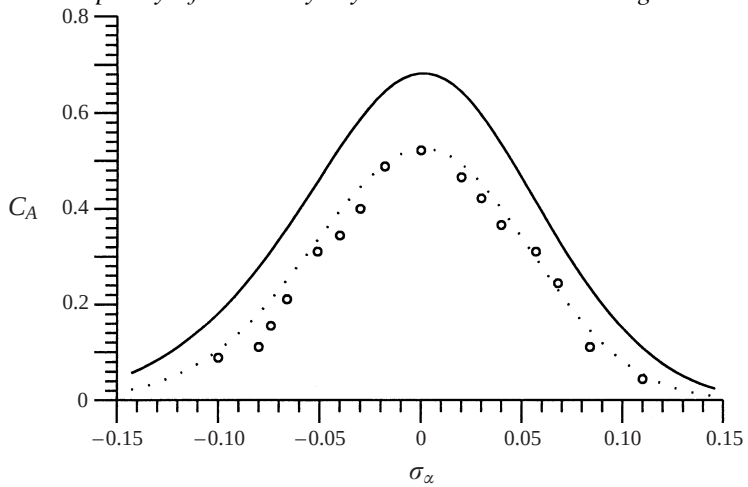

FIGURE 9. Variation of the coupling coefficient C_A with the wavenumber detuning parameter $\sigma_\alpha \equiv (\alpha_w - \alpha)/\alpha$. The solid line represents the results given by the second-order theory, and the dotted line by the 'first-order' theory. The symbols correspond to the measurement of Wiegel & Wlezien (1993).

The second-order theory, while exhibiting the same trend, significantly over-predicts. At this point, one naturally suspects that an error might have occurred in the second-order theory. This suspicion however was dispelled after the present author had spent considerable time checking the derivation as well as the numerical calculations. One may argue that a two-term asymptotic expansion is not necessarily a more accurate approximation than a single-term expansion. Indeed in the case of a regular asymptotic series, for any given value of the small parameter, there is an optimal truncation that will provide the best approximation. But for the present problem, the series is essentially singular (as it will contain terms like $\epsilon^n \log \epsilon$ on proceeding to higher orders), and it is not clear whether an optimal truncation exists or not. A more plausible explanation of the discrepancy probably is the one given by Dietz (1999). He points out that while the initial amplitude is obtained by extrapolation using the N-factor for the Blasius profile, in experiments a slight pressure gradient may exist, (to which the N-factor is known to be very sensitive) and thus the true growth factor may be different. He demonstrates that a small (favourable) pressure gradient within the experiment uncertainty may result in a 30% discrepancy in the estimate of receptivity. Of course such an experimental error also reduces the support for the good agreement shown in the case of the vortical receptivity. To settle this question completely, further experimental and computational investigations are required.

The variation of the efficiency function with the frequency F for the perfectly tuned case ($\alpha_d = 0$) is shown in figure 10. The data reflect the overall efficiency of the acoustic disturbance in generating T-S waves. A comparison with figure 4 indicates that the efficiency function of the vortical receptivity is about 1/6 that of the acoustic receptivity. For the Reynolds numbers considered, this ratio is consistent with the asymptotic estimation that the vortical receptivity is weaker than the acoustic receptivity by a factor $O(R^{-1/8})$. Previous studies suggested that the ratio was about 1/50 (e.g. Crouch 1994), the implication of which is that vortical disturbances are a very ineffective T-S wave generator. This is directly at odds with the laboratory observations that the free-stream turbulence crucially affects the laminar–turbulent transition process caused by T-S waves. Now we find that the vortical receptivity

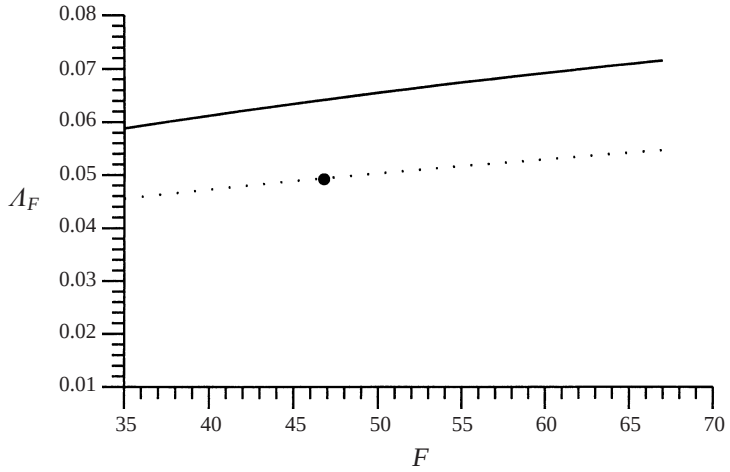

FIGURE 10. Variation of the maximum efficiency function Λ_F (attained when $\alpha_d = 0$) with the forcing frequency F. Wiegel & Wlezien's (1993) experimental result is marked by ●.

is much stronger than was suggested by previous calculations. Indeed since the 1/6 factor could be offset by relatively strong vortical fluctuations in the free stream, they may well be a dominant T-S wave generator in practical situations.

Finally, we would like to point out that in the present work, we used linear solutions for both the mean-flow distortion and the vortical disturbance, with the result that the T-S wave exhibits a linear dependence on h^* and ϵ_c. This is true of course only when the roughness is mild and the free-stream disturbance is weak. In the case of a localized roughness interacting with a sound wave, Zhou, Liu & Blackwelder (1994) observed that when h^* becomes large, the amplitude of the T-S wave is under-predicted by linear theory, implying that the nonlinear effect associated with the mean-flow distortion enhances the receptivity. The same conclusion was reached by Dietz (1999) for the localized vortical receptivity. His experiments also reveal that appreciable deviation from the linear dependence on ϵ_c occurs when the turbulence level exceeds 1%, and more interestingly that further increase in the intensity of the vortical disturbance tends to *weaken* the receptivity. Presumably the above conclusions will also be true for the distributed roughness. The effect of a nonlinear mean-flow distortion on the distributed receptivity could be assessed by using the fully nonlinear steady triple-deck solution, as has been done by Bodonyi *et al.* (1989) for the localized (acoustic) receptivity. But if the roughness height is moderate, a sensible alternative would be to extend the present work to take account of the $O(h^{*2})$ correction. Similarly, by extending our analysis to include the $O(\epsilon_c^2)$ correction, it might be possible to provide a first assessment of the effect of a weakly nonlinear free-stream disturbance on receptivity. If it can be shown that this effect weakens receptivity, we may begin to understand why T-S waves play a less important or no role in the transition process when the free-stream turbulence is sufficiently high.

6. Conclusions

In this paper, we have developed a second-order asymptotic theory for the receptivity of a boundary layer over a wavy wall to the free-stream vortical and acoustic disturbances. It was shown that for distributed roughness, the receptivity actually has a local character, taking place in the $O(R^{-3/16})$ vicinity of the neutral point of the

T-S wave. In this region, the forcing due to the interaction between the unsteady disturbance and the mean-flow distortion is in resonance with the T-S wave, with the result that the latter develops from the small-amplitude response upstream.

The high-Reynolds-number approach adopted in the present work allowed us to calculate the amplitudes of the excited T-S waves in a systematic and self-consistent way. Moreover for the vortical receptivity, it overcame the difficulty of specifying the profile of the disturbance in the free stream, by showing that the detailed profile is largely irrelevant. This made an appropriate comparison between the theory and experiments possible for the first time. A good agreement has been observed. Our results also indicate that the boundary-layer receptivity to the free-stream turbulence is much stronger than suggested by previous calculations.

The theoretical results for the acoustic receptivity have also been compared with the relevant experiments. It is found that our first-order theory agrees very well with measurements, while the second-order theory over predicts. This discrepancy remains to be resolved by further investigations.

The author would like to thank Professor J. T. Stuart, Professor M. Gaster and Dr S. J. Cowley for helpful discussions. Dr M. E. Goldstein and the referees are thanked for their comments and suggestions, which have led to improvement of the paper. The computations were carried out on a computer supported by EPSRC grant GR/L65666/01.

Appendix A. The $O(\epsilon^2)$ correction to the dispersion of T-S waves

The $O(\epsilon^2)$ correction to the T-S wave dispersion can be obtained by seeking the solutions to the quantities with the subscript '3' in each deck and matching, as was described in Smith (1979*a*) and § 3. The final outcome is the equation which determines α_3 and ω_3:

$$
\begin{aligned}
&a\frac{\alpha_3}{\alpha_1}+\eta_0\mathrm{Ai}(\eta_0)\left(\frac{\lambda_0\omega_1}{\alpha_1\gamma_1}-1\right)\frac{\omega_3}{\omega_1}=\frac{\mathrm{i}\lambda_0(\mathrm{i}\alpha_1\lambda_0)^{2/3}}{\gamma_1^2}\left[\frac{\alpha_2}{\gamma_1}+\frac{\gamma_1(\alpha_2-\omega_1)}{\alpha_1^2}-\frac{\gamma_1^2}{\alpha_1}(J_\infty-J_0)\right]\\
&\quad\times\left\{\left(\frac{\omega_2}{\omega_1}-\frac{2}{3}\frac{\alpha_2}{\alpha_1}\right)\eta_0^2\mathrm{Ai}(\eta_0)-\frac{1}{3}\frac{\alpha_2}{\alpha_1}\mathrm{Ai}'(\eta_0)\right\}+\left(\gamma_1 I_2-\frac{\omega_1}{\alpha_1}\right)\left(\frac{\omega_2}{\omega_1}-\frac{2}{3}\frac{\alpha_2}{\alpha_1}\right)\eta_0\mathrm{Ai}(\eta_0)\\
&\quad+\frac{\mathrm{i}\lambda_0(\mathrm{i}\alpha_1\lambda_0)^{2/3}}{\alpha_1^2}\left[\alpha_1\gamma_1(I_2J_0+H_5-H_3)-\omega_1(H_6+J_0+2I_1-I_2)+\frac{\alpha_1^2\alpha_2}{\gamma_1^2}I_2\right]\mathrm{Ai}'(\eta_0)\\
&\quad+\frac{\mathrm{i}\lambda_0(\mathrm{i}\alpha_1\lambda_0)^{2/3}}{\gamma_1^2}\left[-\frac{3(2\alpha_1^2+\beta^2)\alpha_2^2}{2\alpha_1\gamma_1^3}+\frac{(2\alpha_2+\omega_1)\alpha_2}{\alpha_1\gamma_1}-\frac{2\gamma_1\omega_2}{\alpha_1^2}-\frac{(\omega_1^2-2\alpha_2\omega_1)\gamma_1}{\alpha_1^3}\right]\mathrm{Ai}'(\eta_0)\\
&\quad-\frac{\mathrm{i}\lambda_0(\mathrm{i}\alpha_1\lambda_0)^{2/3}}{\alpha_1\gamma_1}\left\{\frac{1}{18}\frac{\alpha_2^2}{\alpha_1^2}(\eta_0^3\mathrm{Ai}'(\eta_0)+3\eta_0^2\mathrm{Ai}(\eta_0)-2\mathrm{Ai}'(\eta_0))\right.\\
&\quad\left.+\frac{1}{2}\left(\frac{\omega_2}{\omega_1}-\frac{\alpha_2}{\alpha_1}\right)\left(\frac{\omega_2}{\omega_1}-\frac{1}{3}\frac{\alpha_2}{\alpha_1}\right)\eta_0^2(\mathrm{Ai}(\eta_0)+\eta_0\mathrm{Ai}'(\eta_0))\right\}\\
&\quad-\left\{\frac{1}{18}\frac{\alpha_2^2}{\alpha_1^2}(-\eta_0^2\mathrm{Ai}'(\eta_0)+2\eta_0\mathrm{Ai}(\eta_0))+\frac{2}{3}\frac{\alpha_2}{\alpha_1}\left(\frac{\omega_2}{\omega_1}-\frac{\alpha_2}{\alpha_1}\right)\eta_0\mathrm{Ai}(\eta_0)\right.\\
&\qquad\left.-\frac{1}{2}\left(\frac{\omega_2}{\omega_1}-\frac{\alpha_2}{\alpha_1}\right)\left(\frac{\omega_2}{\omega_1}-\frac{1}{3}\frac{\alpha_2}{\alpha_1}\right)\eta_0^2\mathrm{Ai}'(\eta_0)\right\},
\end{aligned}
\tag{A 1}
$$

where the constants I_1, I_2 etc. denote the values at $x_0 = 1$ of the integrals defined as follows

$$I_1(x) = \int_0^\infty (U_B - 1)\,\mathrm{d}y, \tag{A 2}$$

$$I_2(x) = \int_0^\infty (U_B^2 - 1)\,\mathrm{d}y, \tag{A 3}$$

$$J_0(x) = -\int_0^a \left(\frac{1}{U_B^2} - \frac{1}{\lambda^2 y^2}\right)\mathrm{d}y + \frac{1}{\lambda^2 a}, \tag{A 4}$$

$$J_\infty(x) = \int_a^\infty \left(\frac{1}{U_B^2} - 1\right)\mathrm{d}y - a; \tag{A 5}$$

$$\begin{aligned}
H_3 &= \int_0^a U_B^2 \left\{\int_a^y \frac{\mathrm{d}y_1}{U_B^2}\right\}\mathrm{d}y + \left\{\int_a^\infty \left(\frac{1}{U_B^2} - 1\right)\mathrm{d}y\right\}\left\{\int_a^\infty (U_B^2 - 1)\mathrm{d}y - a\right\} \\
&\quad + \int_a^\infty (U_B^2 - 1)(y - a)\,\mathrm{d}y - \int_a^\infty U_B^2 \left\{\int_y^\infty \left(\frac{1}{U_B^2} - 1\right)\mathrm{d}y_1\right\}\mathrm{d}y + \tfrac{1}{2}a^2, \\
H_5 &= \int_0^\infty \left(\frac{1}{U_B^2} - 1\right)\left\{\int_0^y U_B^2 \mathrm{d}y_1\right\}\mathrm{d}y - \int_0^\infty y(U_B^2 - 1)\,\mathrm{d}y, \\
H_6 &= 2\int_a^\infty \left(\frac{1}{U_B^3} - 1\right)\mathrm{d}y - \int_a^\infty \left(\frac{1}{U_B^2} - 1\right)\mathrm{d}y + 2\int_0^a \left(\frac{1}{U_B^3} - \frac{1}{\lambda^3 y^3}\right)\mathrm{d}y - \frac{1}{\lambda^3 a^2} - a.
\end{aligned}$$

In all the expressions above, the parameter a is arbitrary provided $a \neq 0$. Since the Blasius profile U_B is a function of the similarity variable $\hat{y} = y/x^{1/2}$, it is convenient, when evaluating these integral, to choose $a = a_0 x^{1/2}$ with a_0 being independent of x. It follows that I_2, J_0 and J_∞ are all proportional to $x^{1/2}$ so that their expansions about x_0 are

$$\left.\begin{aligned}
I_2(x) &= I_2(0) + (\tfrac{1}{2}I_2(0)x_1)R^{-3/16} + \cdots, \\
J_0(x) &= J_0(0) + (\tfrac{1}{2}J_0(0)x_1)R^{-3/16} + \cdots, \\
J_\infty(x) &= J_\infty(0) + (\tfrac{1}{2}J_\infty(0)x_1)R^{-3/16} + \cdots.
\end{aligned}\right\} \tag{A 6}$$

Appendix B. The constants r_0, r_1, r_2 and the function $U_{TS}^{(2)}$

$$\begin{aligned}
r_0 &= \tfrac{1}{3}\mathrm{i}\alpha_1^{-1}(\mathrm{i}\alpha_1\lambda_0)^{2/3}(J_\infty - J_0)\left(\mathrm{Ai}'(\eta_0) + 2\eta_0^2\mathrm{Ai}(\eta_0)\right) - \tfrac{2}{3}\lambda_0^{-1}\gamma_1\eta_0\mathrm{Ai}(\eta_0)I_2 \\
&\quad + \mathrm{i}\omega_1(\mathrm{i}\alpha_1\lambda_0)^{-1}\left\{\tfrac{2}{3}\eta_0\mathrm{Ai}(\eta_0) - \int_{\eta_0}^\infty \mathrm{Ai}(\eta)\mathrm{d}\eta - \frac{2}{3}\frac{(\mathrm{i}\alpha_1\lambda_0)^{5/3}}{\alpha_1^2\gamma_1}[\mathrm{Ai}'(\eta_0) - \eta_0^2\mathrm{Ai}(\eta_0)]\right\} \\
&\quad + \tfrac{2}{3}\mathrm{i}(\alpha_1\gamma_1)^{-1}(\mathrm{i}\alpha_1\lambda_0)^{2/3}\frac{(2\alpha_1^2 + \beta^2)}{\gamma_1^2}\frac{\alpha_2}{\alpha_1}(\mathrm{Ai}'(\eta_0) - \eta_0^2\mathrm{Ai}(\eta_0)) \\
&\quad + \mathrm{i}(\alpha_1\gamma_1)^{-1}(\mathrm{i}\alpha_1\lambda_0)^{2/3}\left\{\frac{2}{9}\frac{\alpha_2}{\alpha_1}\left(\eta_0^3\mathrm{Ai}'(\eta_0) + \mathrm{Ai}'(\eta_0)\right)\right. \\
&\quad \left. + \frac{2}{3}\left(\frac{\omega_2}{\omega_1} - \frac{\alpha_2}{\alpha_1}\right)\eta_0^2(\eta_0\mathrm{Ai}'(\eta_0) + \mathrm{Ai}(\eta_0))\right\} \\
&\quad - \tfrac{2}{3}\lambda_0^{-1}\left\{\left(\frac{\omega_2}{\omega_1} - \frac{5\alpha_2}{3\alpha_1}\right)\eta_0\mathrm{Ai}(\eta_0) + \left(\frac{\omega_2}{\omega_1} - \frac{2\alpha_2}{3\alpha_1}\right)\eta_0^2\mathrm{Ai}'(\eta_0)\right\}.
\end{aligned} \tag{B 1}$$

$$r_1 = \frac{\mathrm{i}(2\alpha_1^2+\beta^2)}{\alpha_1\gamma_1^3}(\mathrm{i}\alpha_1\lambda_0)^{2/3}\left\{\left(\frac{\omega_2}{\omega_1}-\frac{2}{3}\frac{\alpha_2}{\alpha_1}\right)\eta_0^2\mathrm{Ai}(\eta_0)+\frac{2}{3}\frac{\alpha_2}{\alpha_1}\mathrm{Ai}'(\eta_0)\right\}$$
$$+\frac{\mathrm{i}\omega_1(3\alpha_1^2+2\beta^2)}{\alpha_1^2\gamma_1^3}(\mathrm{i}\alpha_1\lambda_0)^{2/3}\mathrm{Ai}'(\eta_0)-\mathrm{i}\alpha_2(\mathrm{i}\alpha_1\lambda_0)^{2/3}\left\{\frac{2\beta^2}{\alpha_1^2\gamma_1^3}+\frac{3(2\alpha_1^2+\beta^2)}{\gamma_1^5}\right\}\mathrm{Ai}'(\eta_0)$$
$$-\lambda_0^{-1}\alpha_1^2\gamma_1^{-1}I_2\int_{\eta_0}^{\infty}\mathrm{Ai}(\eta)\,\mathrm{d}\eta. \tag{B 2}$$

$$r_2 = -\lambda_0^{-1}\left\{\frac{\omega_2}{\omega_1}\eta_0\mathrm{Ai}(\eta_0)+\frac{2}{3}\frac{(\mathrm{i}\alpha_1\lambda_0)^{5/3}}{\alpha_1^2\gamma_1}[\mathrm{Ai}'(\eta_0)-\eta_0^2\mathrm{Ai}(\eta_0)]-2\gamma_1 I_2\int_{\eta_0}^{\infty}\mathrm{Ai}(\eta)\,\mathrm{d}\eta\right\}. \tag{B 3}$$

$$U_{TS}^{(2)} = \left[1-\epsilon\left(\frac{\alpha_2}{\alpha_1}-q_\infty\right)\right]\left\{\int_{\eta_0}^{\eta}\mathrm{Ai}(\eta)\,\mathrm{d}\eta-\frac{\beta_1^2}{\gamma_1^2}\mathrm{Ai}'(\eta_0)Ł(\eta)\right\}$$
$$+\epsilon\left\{\left(\frac{\omega_2}{\omega_1}-\frac{\alpha_2}{\alpha_1}\right)\eta_0(\mathrm{Ai}(\eta)-\mathrm{Ai}(\eta_0))+\frac{1}{3}\frac{\alpha_2}{\alpha_1}(\eta\mathrm{Ai}(\eta)-\eta_0\mathrm{Ai}(\eta_0))\right\}$$
$$-\epsilon\frac{\beta^2}{\gamma_1^2}\left\{\left[\left(\frac{\omega_2}{\omega_1}-\frac{2}{3}\frac{\alpha_2}{\alpha_1}\right)\eta_0^2\mathrm{Ai}(\eta_0)-\frac{2\alpha_1\alpha_2}{\gamma_1^2}\mathrm{Ai}'(\eta_0)\right]Ł(\eta)\right.$$
$$+\left(\frac{\omega_2}{\omega_1}-\frac{\alpha_2}{\alpha_1}\right)\eta_0\mathrm{Ai}'(\eta_0)Ł'(\eta)+\frac{1}{3}\frac{\alpha_2}{\alpha_1}\mathrm{Ai}'(\eta_0)\eta Ł'(\eta)$$
$$\left.+\frac{\displaystyle\int_{\eta_0}^{\infty}\mathrm{Ai}(\eta)\,\mathrm{d}\eta}{\mathrm{Ai}^2(\eta_0)}\left(\frac{\omega_2}{\omega_1}-\frac{2}{3}\frac{\alpha_2}{\alpha_1}\right)\eta_0\mathrm{Ai}'(\eta_0)\mathrm{Ai}(\eta)\right\}. \tag{B 4}$$

Appendix C. Matching between the T-S wave solution and the upstream forced response

To demonstrate more clearly that the T-S wave grows out of the forced response in the pre-resonance region, we now show that these two solutions match in the asymptotic sense. The vortical case will be used for the purpose of illustration. At an arbitrary location in the pre-resonance region, x say, the forced response in the lower deck has expansions similar to (3.62)–(3.65) provided that the T-S wave is excluded and the mean-flow deviation suppressed. Then $\tilde{V}_4$ and $\tilde{V}_5$ would satisfy (3.98) and (3.104), and their solutions can be written as (3.99) and (3.105) respectively, provided of course that A and q_2 are set to zero, and λ_0 is replaced by λ. The solutions in the upper and main decks are similar to those given in § 3.1 and § 3.3. Then on applying the boundary and matching conditions, we find that q_4 and q_5 are determined by

$$q_4 = \frac{\lambda F_v}{\Delta(\lambda)}\,\mathrm{e}^{\mathrm{i}\alpha_d x_1}, \tag{C 1}$$

$$q_5 = \left\{\left(\frac{\omega_1}{\alpha_1}-\gamma_1 I_2(x)+\left(1+\frac{\alpha_1^2}{\gamma_1^2}\right)\frac{\alpha_2}{\alpha_1}\right)-\frac{\Delta_1(\lambda)}{\Delta(\lambda)}\right\}q_4+\frac{\lambda F_c}{\Delta(\lambda)}\,\mathrm{e}^{\mathrm{i}\alpha_d x_1}, \tag{C 2}$$

where $\Delta(\lambda)$ and $\Delta_1(\lambda)$ are defined by (3.75) and (3.87) respectively with λ_0 being understood as λ, the dependence on which is through η_0, I_2, J_0 and J_∞. A Taylor

expansion of $\Delta(\lambda)$ about λ_0 shows that as $x \to x_0$,

$$q_4 \to \frac{\lambda_0^2 F_v}{\mathrm{i}\alpha_1 b(\lambda - \lambda_0)} = R^{3/16}(N/\sigma)(-x_1)^{-1}\,\mathrm{e}^{\mathrm{i}\alpha_d x_1}, \tag{C 3}$$

indicating that q_4 matches to A; see (3.113). Similarly, expanding $\Delta_1(\lambda)$, and I_2, J_∞ and using the relations that

$$\Delta_1(\lambda_0) = 0, \quad \frac{\partial I_2}{\partial \lambda}(\lambda_0) = -I_2(0)/\lambda_0, \quad \frac{\partial J_0}{\partial \lambda}(\lambda_0) = -J_0(0)/\lambda_0, \quad \frac{\partial J_\infty}{\partial \lambda}(\lambda_0) = -J_\infty(0)/\lambda_0,$$

we find that

$$q_5 \to \left\{ \left\{ \frac{\omega_1}{\alpha_1} - \gamma_1 I_2(0) + \left(1 + \frac{\alpha_1^2}{\gamma_1^2}\right)\frac{\alpha_2}{\alpha_1} - \frac{\lambda_0 \Delta_1'(\lambda_0)}{\mathrm{i}\alpha_1 b} \right\} \frac{N}{\sigma} - \frac{\lambda_0^2 F_c}{\mathrm{i}\alpha_1 \lambda_1 b} \right\} R^{3/16}(-x_1)^{-1}\,\mathrm{e}^{\mathrm{i}\alpha_d x_1}. \tag{C 4}$$

A comparison with (3.115) suggests that q_5 matches to q_2 if

$$\left\{ \frac{\omega_1}{\alpha_1} - \gamma_1 I_2(0) + \left(1 + \frac{\alpha_1^2}{\gamma_1^2}\right)\frac{\alpha_2}{\alpha_1} \right\} b - \frac{\lambda_0 \Delta_1'(\lambda_0)}{\mathrm{i}\alpha_1} = \lambda_0(r_0 + r_2). \tag{C 5}$$

The above identity is verified by a direct calculation using (3.87).

REFERENCES

Bodonyi, R. J., Welch, W. J. C., Duck, P. W. & Tadjfar, M. 1989 A numerical study of the interaction between unsteady free-stream disturbances and localized variations in surface geometry. *J. Fluid Mech.* **209**, 285–308.

Brown, S. N. & Stewartson, K. 1973 On the propagation of disturbances in a laminar boundary layer. *Math. Proc. Camb. Phil. Soc.* **73**, 493–514.

Choudhari, M. 1993 Boundary-layer receptivity due to distributed surface imperfections of a deterministic or random nature. *Theor. Comput. Fluid Dyn.* **4**(3), 101–117.

Choudhari, M. 1994 Distributed acoustic receptivity in laminar flow control configurations. *Phys. Fluids* **6**, 489–506.

Choudhari, M. 1996 Boundary-layer receptivity to three-dimensional unsteady vortical disturbances in free stream. *AIAA Paper* 96-0181.

Choudhari, M. & Streett, C. L. 1992 A finite Reynolds number approach for the prediction of boundary-layer receptivity in localized regions. *Phys. Fluids* **4**, 2495–2514.

Crouch, J. D. 1992*a* Localized receptivity of boundary layers. *Phys. Fluids* **4**, 1408–1414.

Crouch, J. D. 1992*b* Non-localized receptivity of boundary layers. *J. Fluid Mech.* **244**, 567–581.

Crouch, J. D. 1994 Distributed excitation of Tollmien–Schlichting waves by vortical free-stream disturbances. *Phys. Fluids* **6**, 217–223.

Dietz, A. J. 1996 Distributed boundary layer receptivity to convected vorticity. *AIAA Paper* 96-2083.

Dietz, A. J. 1998 Boundary-layer receptivity to transient convected disturbances. *AIAA J.* **36**, 1171–1177.

Dietz, A. J. 1999 Local boundary-layer receptivity to a convected free-stream disturbance. *J. Fluid Mech.* **378**, 291–317.

Duck, P. W., Ruban, A. I. & Zhikharev, C. N. 1996 Generation of Tollmien–Schlichting waves by free-stream turbulence. *J. Fluid. Mech.* **312**, 341–371.

Goldstein, M. E. 1983 The evolution of Tollmien–Schlichting waves near a leading edge. *J. Fluid Mech.* **127**, 59–81.

Goldstein, M. E. 1985 Scattering of acoustic waves into Tollmien–Schlichting waves by small streamwise variations in surface geometry. *J. Fluid Mech.* **154**, 509–529.

Goldstein, M. E. & Hultgren, L. S. 1987 A note on the generation of Tollmien–Schlichting waves by sudden surface-curvature change. *J. Fluid. Mech.* **181**, 519–525.

Gulyaev, A. N., Kozlov, V. E., Kuznetson, V. R., Mineev, B. I. & Sekundov, A. N. 1989 Interaction of laminar boundary layer with external turbulence. *Izv. Akad. Nauk SSSR Mekh. Zhid. Gaza* **6**, 700–710.

HALL, P. & SMITH, F. T. 1984 On the effects of non-parallelism, three-dimensionality and mode interaction in nonlinear boundary-layer stability. *Stud. Appl. Maths* **71**, 91–120.

KENDALL, J. M. 1985 Experimental study of disturbances produced in pre-transitional laminar boundary layer by weak free stream turbulence. *AIAA Paper* 85-1695.

KENDALL, J. M. 1990 Boundary-layer receptivity to free-stream turbulence. *AIAA Paper* 90-1504.

KERSCHEN, E. J. 1991 Linear and nonlinear receptivity to vortical free-stream disturbances. In *Boundary Layer Stability and Turbulence* (ed. D. C. Reda, H. L. Reed & R. K. Kobayashi) ASME FED, vol. 114, pp. 43–48.

KOVASZNAY, L. S. G. 1953 Turbulence in supersonic flow. *J. Aero. Sci.* **20**, 657–682.

LEIB, S. J., WUNDROW, D. W. & GOLDSTEIN, M. E. 1999 Effect of free-stream turbulence and other vortical disturbances on a laminar boundary layer. *J. Fluid Mech.* **380**, 169–203.

LIN, C. C. 1946 On the stability of two-dimensional parallel flows. Part 3. Stability in a viscous fluid. *Q. Appl. Maths.* **3**, 277–301.

MORKOVIN, M. V. 1969 Critical evaluation of transition from laminar to turbulent shear layers with emphasis on hypersonically travelling bodies. AFFDL-TR 68-149. US Air Force Flight Dynamics Laboratory, Wright Patterson Air Force Base, Ohio.

RESHOTKO, E. 1976 Boundary layer stability and transition. *Ann. Rev. Fluid Mech.* **8**, 311–349.

RUBAN, A. I. 1983 Nonlinear equation for the amplitude of Tollmien–Schlichting waves in the boundary layer. *Izv. Akad. Nauk. SSSR Mekh. Zhid. Gaza* **6**, 60–67.

RUBAN, A. I. 1984 On Tollmien–Schlichting wave generation by sound. *Izv. Akad. Nauk. SSSR Mekh. Zhid. Gaza* **5**, 44 (in Russian; English Translation: *Fluid Dyn.* **19**, 709–716 (1985)).

RUBAN, A. I., DUCK, P. W. & ZHIKHAREV, C. N. 1996 The generation of Tollmien–Schlichting waves by freestream vortical perturbations. *AIAA Paper* 96-2123.

RYZHOV, O. S. & TERENT'EV, E. D. 1977 On unsteady boundary layer with self-induced pressure. *Prikl. Mat. Makh.* **41**(6), 277–301.

SMITH, F. T. 1979*a* On the nonparallel flow stability of the Blasius boundary layer. *Proc. R. Soc. Lond.* A **366**, 91–109.

SMITH, F. T. 1979*b* Nonlinear stability of boundary layers for disturbances of various sizes. *Proc. R. Soc. Lond.* A **368**, 573–589.

TAM, C. K. W. 1981 The excitation of Tollmien–Schlichting waves in lower subsonic boundary layers by free-stream sound waves. *J. Fluid Mech.* **109**, 483–501.

TERENT'EV, E. D 1981 The linear problem of a vibrator in a subsonic boundary layer. *Prikl. Math. Mech.* **45**, 1049–1055.

WIEGEL, M. & WLEZIEN, R. W. 1993 Acoustic receptivity of laminar boundary layers over wavy walls. *AIAA Paper* 93-3280.

WU, X. 1999 Generation of Tollmien–Schlichting waves by convecting gusts interacting with sound. *J. Fluid Mech.* **397**, 285–316.

ZHIGULEV, V. N. & TUMIN, A. M. 1987 *Origin of Turbulence.* NAUKA, Novosibirsk.

ZHOU, M. D., LIU, D. P. & BLACKWELDER, R. F. 1994 An experimental study of receptivity of acoustic waves in laminar boundary layers. *Exps. Fluids* **17**, 1–9.